Ecotoxicology and Environmental Safety 211 (2021) 111926

Contents lists available at ScienceDirect

Ecotoxicology and Environmental Safety

journal homepage: www.elsevier.com/locate/ecoenv

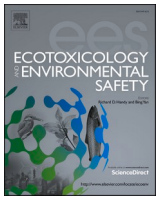

Groundwater fluoride chemistry and health risk assessment of multi-aquifers in Jilin Qianan, Northeastern China

Oluwafemi Adewole Adeyeye [a,b,c,d], Changlai Xiao [a,b,c,*], Zhihao Zhang [a,b,c], Achivir Stella Yawe [a,b,c,d], Xiujuan Liang [a,b,c,*]

[a] Key Laboratory of Groundwater Resources and Environment, Jilin University, Ministry of Education, Changchun 130021, China
[b] National Local Joint Engineering Laboratory of In-situ Conversion, Drilling and Exploitation Technology for Oil Shale, Changchun 130021, China
[c] College of New Energy and Environment, Jilin University, Changchun 130021, China
[d] Global Geosolutionz, Typesetters Biz Complex, Department of Geology, Ahmadu Bello University, Zaria 810107, Nigeria

ARTICLE INFO

Edited by: Dr Fernando Barbosa

Keywords:
Fluoride
Health risk assessment
Multi-aquifers
Jilin Qianan

ABSTRACT

Groundwater from deep confined aquifers is often recommended for use because of it's low fluoride health risk. Thus, this study appraised groundwater fluoride hydrochemistry in a multi-aquifer system in Jilin Qianan to determine the non-carcinogenic health risk liable from exploiting the respective aquifers. 124 samples collected from the tertiary confined aquifer (N), quaternary confined aquifer (Q_1), and quaternary phreatic aquifer (Q_3) during surveys in 2001 and 2017 was analyzed using hydrochemical, statistical, spatial, and health risk assessment methods. Results show that the dominant water facies in the respective aquifer layers was $Na+K–HCO_3+CO_3$ except in Q_1, where $Ca+Mg – HCO_3 + CO_3$ was marginally dominant. Fluoride concentrations outside the recommended guideline occurred in all the aquifers except N, where concentrations were optimum. The mean fluoride concentration of groundwater in the aquifers was of the order Q_3 (2017) > Q_3 (2001) > Q_1 > N (mean 2.09, 2.03, 1.41 and 0.75 mg/L with 51.85%, 57.44%, 36.36% and 0% occurring beyond recommended guideline values respectively). Silicate weathering, cation exchange, and fluorite dissolution in an alkaline environment were the significant fluoride contributing processes. Evaporation and MgF^+ complex additionally influenced Q_1 and Q_3 (2017). The total hazard quotient (THQ) from oral and dermal pathways shows fluoride health risks in the order: infant > children > adult. The associated risks likely from using water in the respective aquifer layers is of the order Q_3 (2017) > Q_3 (2001) > Q_1 > N. The mean groundwater fluoride in 2017 was marginally higher than that of 2001 (2.09>2.03 mg/L respectively) although the percentage of age group members disposed to fluoride risk from using water from Q_3 decreased from 2001 to 2017. Knowledge of local hydrogeology in exploiting deep groundwater free of fluoride pollution and on-site defluoridation treatment of groundwater was recommended in the study area and other areas with similar characteristics.

1. Introduction

Fluorine is widespread in the environment. In water, it is safe for drinking within the limits of 0.5–1.5 mg/l according to the recommended guidelines (WHO, 2017; Yousefi et al., 2018a). At concentrations below/above this recommendation, fluoride becomes detrimental to health and is referred to as a double-edged sword (Gazzano et al., 2010; Goldberg, 2018). At lower concentration, water consumers are susceptible to dental carries while at concentrations higher than stipulated, it can cause dental fluorosis, skeletal fluorosis, crippling fluorosis, and detrimental effects on the kidneys (Demelash et al., 2019; Dharmaratne, 2019; Dissanayake and Chandrajith, 2019; Malago, 2017). Excessive fluoride intake has also been linked to fertility, infertility, abortion, and hypertension (Yousefi et al., 2017, 2018b). Ingestion and dermal absorption of water are the main intake pathways of trace elements in the environment (Dhiman and Keshari, 2006; Zhai et al., 2017).

Around 200 million people are estimated worldwide to be affected by fluorosis (Ayoob and Gupta, 2006). In Asia, for instance, it is estimated that a population of 25 million in Pakistan (Farooqi et al., 2007), 22–45 million in China (J. Li et al., 2020; Wang et al., 2002), and 66 million in India (Mukherjee and Singh, 2018) are affected by high

* Corresponding authors at: Key Laboratory of Groundwater Resources and Environment, Jilin University, Ministry of Education, Changchun 130021, China
E-mail addresses: xcl2822@126.com (C. Xiao), lax64@126.com (X. Liang).

https://doi.org/10.1016/j.ecoenv.2021.111926
Received 29 October 2020; Received in revised form 23 December 2020; Accepted 8 January 2021
Available online 17 January 2021
0147-6513/© 2021 The Authors. Published by Elsevier Inc. This is an open access article under the CC BY-NC-ND license (http://creativecommons.org/licenses/by-nc-nd/4.0/).

fluoride in water. There is thus a need to understand fluoride source and mobilization mechanism in the environment for water resources management purposes (Amini et al., 2016; Emenike et al., 2018; Subba Rao et al., 2016). The occurrence of fluoride in groundwater depends on temperature, pH, the influence of complex or precipitating ions and colloids, the solubility of fluoride bearing minerals, anion exchange capacity of aquifer material, aquifer type, and residence time (Apambire et al., 1997; Reddy et al., 2010; Rezaei et al., 2017). Anthropogenic activities also exacerbate fluoride contamination in the environment (Farooqi et al., 2007; Jia et al., 2019).

In China, the brackish waters in the northern coastal aquifers, the iron-rich soils in the south, and the sodic groundwaters of the arid/semi-arid areas of the north have been identified as geochemical environments favourable to geogenic fluoride enrichment (Jia et al., 2018; Wen et al., 2013). The groundwater of Jilin Qianan, like most of the Songnen plain of northeastern China, is known to have deleteriously high fluoride concentration, with the mechanism of enrichment being related primarily to weathering of parent rocks and secondarily to leaching, desorption, and carbonate sedimentology under alkaline conditions (Jia et al., 2018; M. Li et al., 2019; Wen et al., 2013; Xibei, 2007; Zhang et al., 2003; Zhiwu, 2009). The fluoride health risk associated with ingestion of such water has been considered mostly at regional scales (Zhang et al., 2003; Zhang et al., 2017), and studies on smaller scales focus on the unconfined phreatic aquifer (Xibei, 2007; Zhang et al., 2003). Deeper aquifers have also been recommended for use because of observed lower fluoride content than the shallow phreatic aquifer (Jia et al., 2019; Wen et al., 2013; Xibei, 2007; Zhang et al., 2003). However, there is a gradual trend of contamination of deep aquifers in response to natural and anthropogenic influences (Chen et al., 2017; Jia et al., 2019; Zhan and Bian, 2006). Qian et al. (2020) estimated that nearly 60% of inflow into the confined aquifer in the Yinchuan region of north central China originated from leakage from the phreatic aquifer, although minimal (0.2%) compared to the volume of water in the confined aquifer storage. In Jilin Qian'an, like most of western Jilin Province, poorly managed drill wells with hole density ranging from 1.32 to 10 holes per square kilometer has increased the hydraulic connection between the phreatic aquifer and the unconfined aquifer leading to pollution of the confined water (M. Li et al., 2020; Liao and Lin, 2004). It is thus essential to consider the health risk associated with ingesting waters from these deeper aquifers.

Additionally, approximately 82% of endemic fluoride villages in China have implemented defluoridation projects by 2010 (Zhao et al., 2013), with the main defluoridation methods practiced being physical treatments, chemical reduction, and modification at the source point which is the most widespread (Zhang et al., 2017). Source point modification may also involve the drilling of deep wells into aquifers that often have a lower concentration of fluoride, and many government-sponsored public water supply systems in some areas plagued by high fluoride in water exploit this technique (Fawell et al., 2006; Jia et al., 2019). Wang et al. (2019) emphasized the need for a detailed monitoring system to track changes in environmental conditions and exposure to fluoride in children. This study, therefore, undertakes an aquifer-based fluoride health risk assessment of groundwater in the multi-aquifers in Jilin Qianan. The main objectives of this research are to (1) Determine the groundwater chemistry of the respective aquifer layers; (2) Determine the levels of fluoride in the aquifers in the area; (3) Delineate fluoride source and mobilization mechanism in the study area; (4) Determine the aquifer-based non-carcinogenic fluoride health risks of groundwater; (5) Assess the temporal variation of groundwater fluoride in an aquifer in 2001 and 2017 respectively. The results from this study will aid water resources managers in appraising the viability of confined deeper aquifers as an alternative to unconfined aquifers in controlling endemic fluorosis in China and the rest of the world.

2. Study area

Jilin Qianan, with a population of about 301,981 people, is a county located in Northeastern China, the northwestern part of Jilin province, and the central part of the Songnen Plain (Fig. 1). It bounded approximately by longitudes 123°21 '16 – 124°22' 50 " E and latitudes 44°37 '47" – 45°18' 08" N, covering an area of 3617.24 km^2, with a total cultivated land area of 169.35 km^2. The study area belongs to the arid and semi-arid continental monsoon climate in the middle temperate zone. According to the observation data of the Qianan meteorological station, the average temperature for many years is 4.6 ℃. Meteorological data from the study area indicate that the average annual precipitation in the area is 415.53 mm and is concentrated mainly in June to September, accounting for more than 80% of the annual precipitation. The lowest occurrence was in 2001, with precipitation of 220.3 mm. The perennial average evaporation was 1849.01 mm. The annual evaporation rate is mainly concentrated in April to September, during which the evaporation rate was about 80% of the annual evaporation rate. Geomorphologically, the study area surface is highly salinized, with light wetland formation or slight marsh – wetland formation, perennial water accumulation or seasonal water accumulation, and an elevation of 120–138 m above sea level (masl), which decreases from southeast to northwest and northeast respectively.

Jilin Qianan is located in the central depression zone of Songnen low plain with Mesozoic and Cenozoic strata widely distributed in the study area. The stratigraphy of the area, as obtained from borehole data, has at its base a cretaceous system characterized by mudstone and glutenite of the Mingshui Formation (K_2m). It is widely distributed in the area, with a buried depth of about 275 m and a single layer thickness greater than 59.84 m. Overlying it is the upper Tertiary Da'an Group (Nd) and Taikang Group (Nt). The Da'an Formation (Nd) is widely distributed and comprises fine sands, sandstone, argillaceous conglomerate, and glutenite. The Taikang Formation (Nt) is widely distributed and is composed of conglomerate, silty mudstone, and mudstone, generally buried at a depth of 25–108 m with a thickness range of 83–93 m (Fig. 1b, Supplementary Data, Fig. S1).

Quaternary system (Q) mainly developed in this area are Baitushan Formation of lower Pleistocene, Daqinggou Formation of middle Pleistocene, Guxiangtun formation of upper Pleistocene and Holocene strata, with a total thickness of 25–95 m. The Baitushan Formation (Q_1^b) with a lithology of sand, gravel, relatively loose, partially sandwiched thin layer of clay lenses. The Daqinggou Formation (Q_2^d) of the middle Pleistocene is widely distributed and is dominated by lacustrine facies. Silty loam, sandy loam, and sand lenses make up its lithology. The Guxiangtun Formation ($Q_{3\ gal}$) is widely distributed in the area, and it is a loose accumulation layer mainly composed of gravel, sand, sandy loam, and loessial loam. The Holocene is composed of aeolian deposit (Q_4^{eol}) and lacustrine deposits (Q_4^l) and is mainly distributed in the northwest, north-central and northeastern parts of the study area. Lithologies present include sand, sandy loam, loam, and gravel. In terms of hydrogeology, Guxiangtun Formation and Mingshui Formation are aquitards. The Holocene aquifer is phreatic while the others are confined (Fig. 1).

3. Methodology

3.1. Sample collection and analysis

Forty-seven samples from the phreatic quaternary aquifer (Q_3), forty-four from the quaternary confined aquifer (Q_1), and six from the tertiary confined aquifer (N) were collected based on well location, well-depth, and local hydrogeology by the Jilin Water Resources Bureau for groundwater quality and fluoride monitoring purposes at the end of the second quarter, 2001. The authors similarly collected an additional twenty-seven (27) phreatic groundwater samples for the same purpose in the fourth quarter of 2017, totalling one hundred and twenty-four (124) groundwater samples collected and analyzed from Jilin Qianan

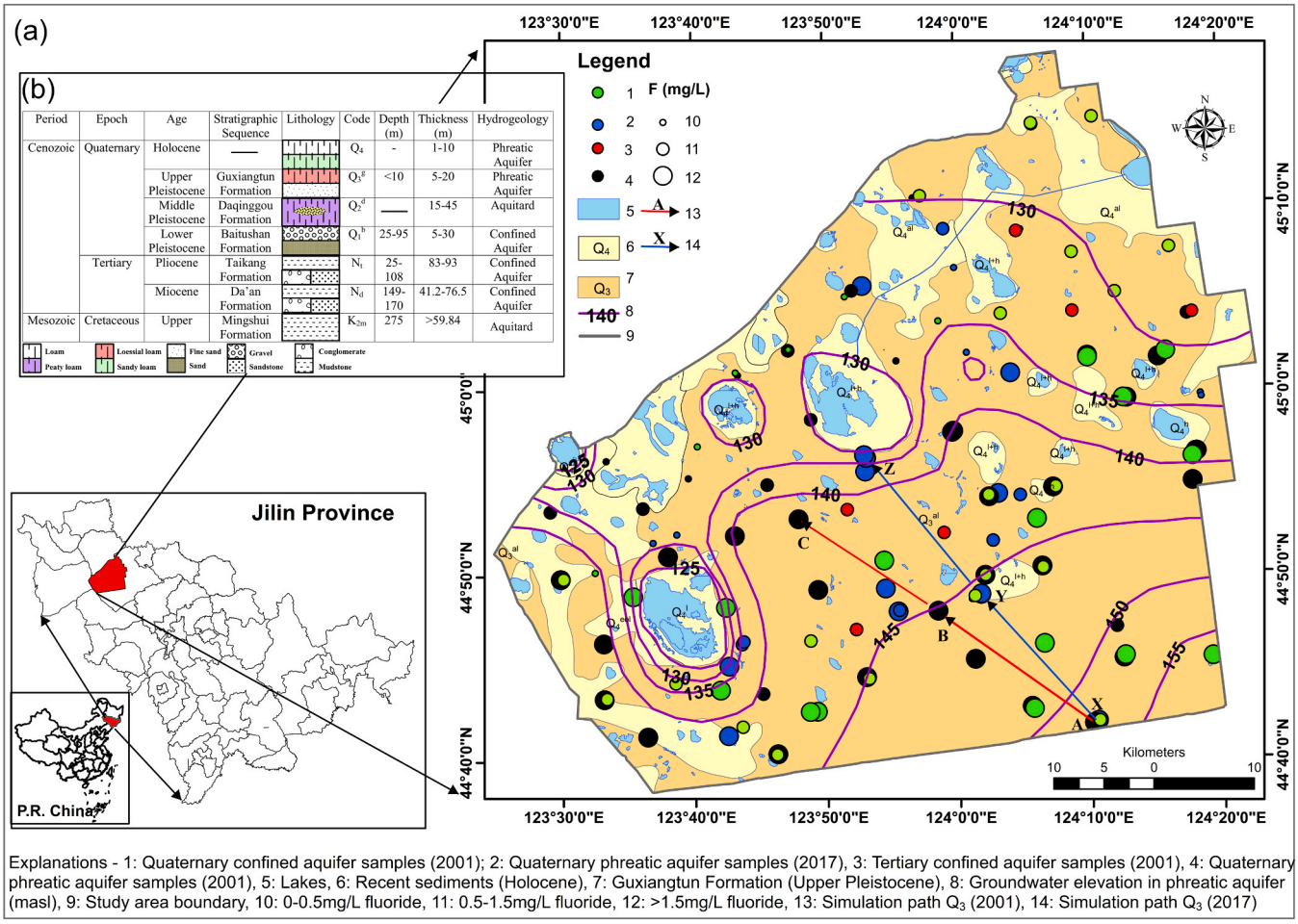

Period	Epoch	Age	Stratigraphic Sequence	Lithology	Code	Depth (m)	Thickness (m)	Hydrogeology
Cenozoic	Quaternary	Holocene	——		Q_4	-	1-10	Phreatic Aquifer
		Upper Pleistocene	Guxiangtun Formation		Q_3^g	<10	5-20	Phreatic Aquifer
		Middle Pleistocene	Daqinggou Formation		Q_2^d	——	15-45	Aquitard
		Lower Pleistocene	Baitushan Formation		Q_1^b	25-95	5-30	Confined Aquifer
	Tertiary	Pliocene	Taikang Formation		N_t	25-108	83-93	Confined Aquifer
		Miocene	Da'an Formation		N_d	149-170	41.2-76.5	Confined Aquifer
Mesozoic	Cretaceous	Upper	Mingshui Formation		K_{2m}	275	>59.84	Aquitard

Loam, Peaty loam, Loessial loam, Sandy loam, Fine sand, Sand, Gravel, Sandstone, Conglomerate, Mudstone

Fig. 1. (a) Location map of the area showing sampling points, geology, groundwater elevation, and fluoride concentration; (b) Lithostratigraphy and hydrogeology of the area.

for this study. The Chinese National Standard procedure for sampling, which involves collecting two water samples per location, was followed (NEPS-PRC, 2009). Plastic bottles were thoroughly rinsed with water from the well to be sampled, and samples used for cation analysis were acidified to a pH of about two using few drops of concentrated HNO_3. The sample for anion determination was taken directly to the laboratory without acidifying. Pony Testing International Group did all analyses in Changchun following Standard Examination Methods for Drinking Water (National Standardization Administration of China, 2007a; 2007b). The major cations (K^+, Na^+, Ca^{2+}, Mg^{2+}, Fe^{3+}) were analyzed using inductively coupled plasma atomic emission spectrometry (ICP-AES). An ion chromatograph measured F^-, Cl^-, NO_3^-, and SO_4^{2-}. Total hardness (TH) ($CaCO_3$ hardness) was measured by Na_2EDTA titrimetric method and HCO_3^- by acid-base titration. The temperature and pH were measured in-situ using a calibrated EC/pH metre (HANNA, HI99131). An electric blast-drying oven, along with an electronic analytical balance (vapour-drying method), was used to measure TDS. The reliability of the water sample analysis was confirmed as all the samples had errors less than 10% when assessed using the ionic balance equation.

3.2. Geochemical modelling

The dominant ionic phases/water facies were classified using the Piper tri-linear diagram (Piper, 1944). The PHREEQC programming bundle (Parkhurst and Appelo, 1999) was used to estimate the degree of saturation of fluoride-related minerals (calcite, fluorite, aragonite, gypsum, halite, and dolomite, respectively) in all the water sampled. The saturation indices (SI), which indicate the thermodynamic tendency of minerals to dissolve or precipitate was computed using Eq. (1).

$$SI = Log\left(IAP/K_{sp}\right) = LogIAP - LogK_{sp} \quad (1)$$

Where SI means saturation index, IAP is the ion activity product of the dissociated chemical species in solution, and K_{sp} is the equilibrium solubility product for the chemical involved at sample temperature. Based on the value of the SI, the saturation states are recognized as in equilibrium when SI = 0, undersaturation when SI < 0, and oversaturation when SI > 0.

Inverse modelling of groundwater chemical evolution along two flow paths along the Q_3 in 2001 and 2017 was similarly carried out using PHREEQC (Fig. 1). Based on the groundwater flow path and hydrological condition, paths A–C (2001) and X–Z (2017) were selected. The major ions (Na/Mg/Ca and $HCO_3/Cl/SO_4$) and the trace element (F) were employed in the simulation. The representative mineral phases calcite, dolomite, gypsum, and halite, which are characteristic of the study area, were selected. Additionally, because of the wide distribution of clay minerals in the study area that makes cation exchange likely, the openness of the system, and strong evaporation tendency, the model also included CaX_2/NaX, $CO_2(g)$, and $H_2O(g)$ phases (Du et al., 2009; M. Li et al., 2019).

3.3. Statistical and spatial analysis

Descriptive statistics of groundwater physicochemical parameters was done using Microsoft Excel 2010 software package. The software Statistical Package for Social Sciences (SPSS) v. 16 was used for correlation analysis between fluoride and other groundwater properties to identify the principal factors that affect the concentration of fluoride in the water.

3.4. Human health risk assessment

To assess the probable adverse effect of fluoride from water intake over a long period, the tested and widely used model of the United States Environmental Protection Agency was adopted (US EPA, 1989). The study area was grouped into three categories: infants (<6 months), children (>6months ≤ 17years), and adults (>17 years) (Yin et al., 2020; Zhai et al., 2017). Oral and dermal intake pathways were considered because they are the most dominant potential exposure pathways to groundwater contaminants in daily life (Emenike et al.,

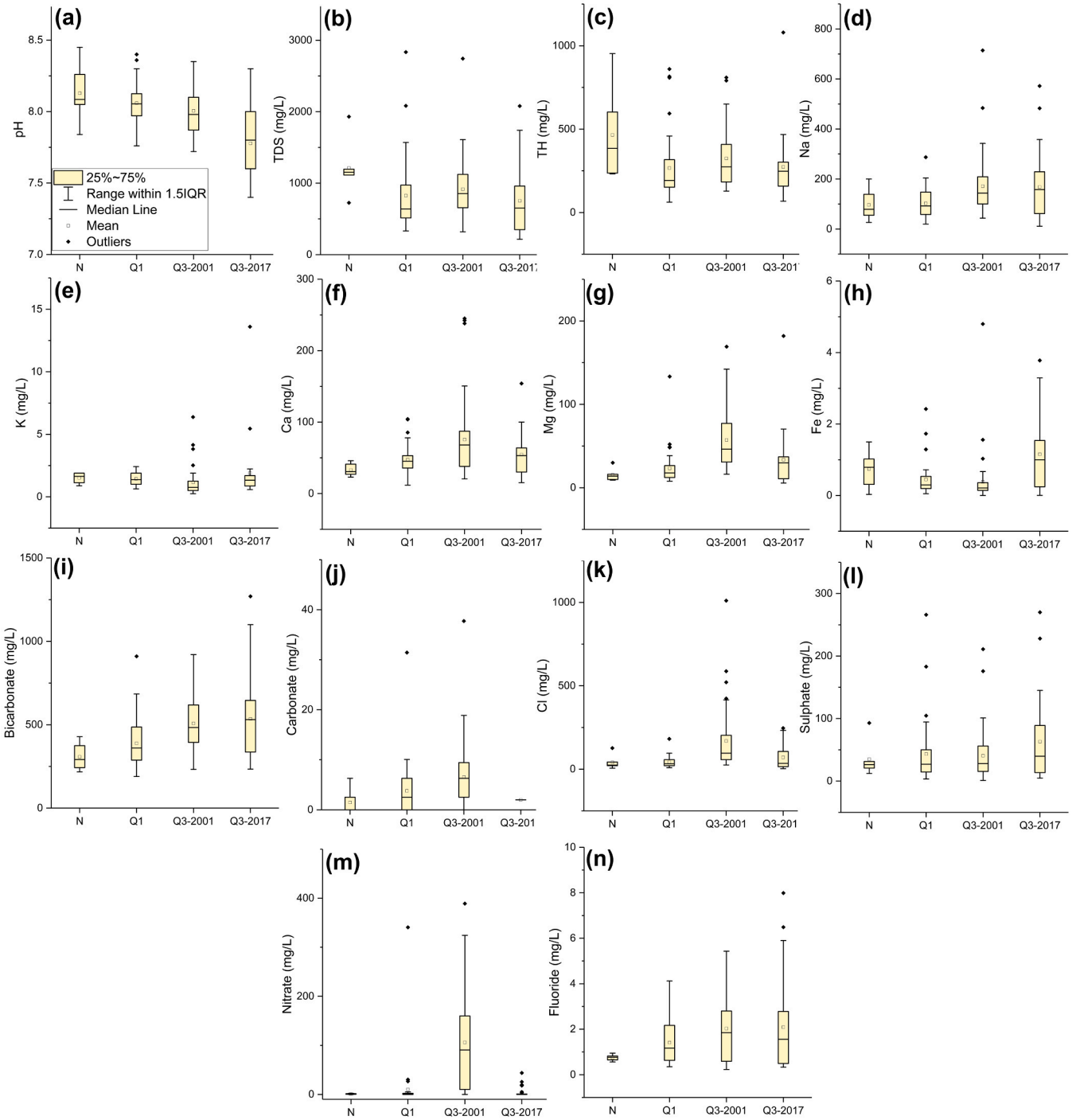

Fig. 2. Box plots for the groundwater physicochemical parameters: (a) pH, (b) TDS, (c) TH, (d) Na, (e) K, (f) Ca, (g) Mg, (h) Fe, (i) bicarbonate, (j) carbonate, (k) Cl, (l) sulphate, (m) nitrate, (n) fluoride. N, Q_1, Q_3–2001 and Q_3–2017 refers to water from tertiary confined aquifer, quaternary confined aquifer, quaternary phreatic aquifer (2001) and quaternary phreatic aquifer (2017) respectively.

2018; Yin et al., 2020). The non-carcinogenic risk through the oral pathway was determined using Eqs. (2) and (3), while the non-carcinogenic risk due to dermal intake was determined using Eqs. (4) and (5). The total hazard quotient of non-carcinogenic risk due to fluoride (THQ) was obtained using Eq. (6).

$$EDI_{oral} = C_w \times IR \times EF \times ED/BW \times AT \quad (2)$$

$$HQ_{oral} = EDI_{oral}/RfD_{oral} \quad (3)$$

Where EDI_{oral} means estimated daily intake through the oral pathway, C_w means the concentration of fluoride in water (mg/L), IR means ingestion rate of drinking water (L/day), EF means resident exposure frequency (days), ED means exposure duration (years), BW means bodyweight (Kg), AT means exposure time (days), HQ_{oral} means hazard quotient from the oral pathway, and RfD_{oral} means reference dose of fluoride due to oral intake of water [mg/(Kg x day)]. The calculation parameters used for this study are listed in Table S1.

$$EDI_{dermal} = C_w \times SA \times K \times ED \times EF \times ET \times CF/BW \times AT \quad (4)$$

$$HQ_{dermal} = EDI_{dermal}/RfD_{dermal} \quad (5)$$

Where EDI_{dermal} means estimated daily intake through the dermal pathway, C_w means the concentration of fluoride in water (mg/L), SA body surface area (cm^2), K means dermal permeability coefficient of water (cm/h), EF means resident exposure frequency (days), ED means exposure duration (years), ET means water exposure time (h/day), CF means conversion factor (L/cm^3), BW means bodyweight (Kg), AT means exposure time (days), HQ_{dermal} means hazard quotient from the dermal pathway, and RfD_{dermal} means reference dose of fluoride due to dermal contact with water [mg/(Kg x day)].

$$THQ = HQ_{oral} + HQ_{dermal} \quad (6)$$

Where THQ means total hazard quotient due to oral intake and dermal contact, respectively.

4. Results and discussion

4.1. Groundwater hydrochemistry

The summary of physicochemical characteristics is given in Fig. 2 and Table S2 (Supplementary Material). The groundwater in aquifers in the study area is generally slightly alkaline ranging from 7.40 in Q_3 (2017) to 8.45 in N. (Fig. 3).

The major cation composition of groundwater in the aquifers analyzed is of order $Na^+ > Ca^{2+} > Mg^{2+} > K^+$. The anionic magnitude in N and Q_3 (2017) is respectively of the order $HCO_3^{2-} > Cl^- > SO_4^{2-} > NO_3^-$, while in the Q_1, the anionic dominance was of the order $HCO_3^{2-} > SO_4^{2-} > Cl^- > NO_3^-$. In the Q_3 aquifer in 2001(Q_3 2001), the anionic dominance is

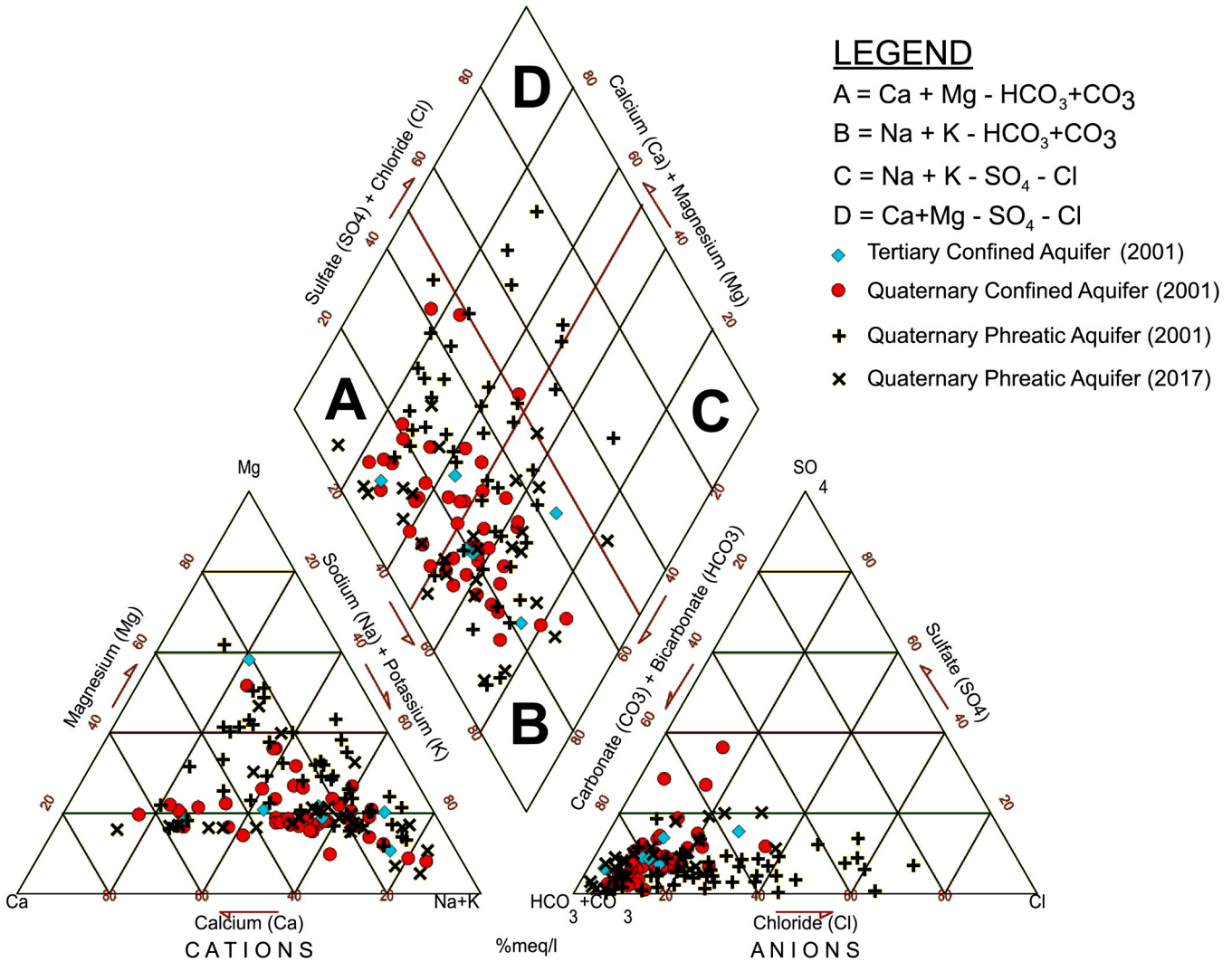

Fig. 3. Piper plot showing groundwater hydrochemical facies characterization.

of the order $HCO_3^{2-} > Cl^- > NO_3^- > SO_4^{2-}$.

In the tertiary aquifer, Na+K – HCO_3+CO_3 water facies dominates (66.67%), followed by Ca+Mg – HCO_3 + CO_3 (47.73%) (Fig. 2). The groundwater is slightly alkaline, with pH ranging from 7.8 to 8.45 (average 8.13). The pH falls within the recommended guidelines (WHO, 2017). Total dissolved solids (TDS) ranged from 725.66 to 1920 mg/L (average 1212.28 mg/L) with 83.33% being brackish and exceeding the recommended guidelines of 1000 mg/L (WHO, 2017). The high TDS of this confined groundwater may be due to infiltration from phreatic sources common in the Songnen plain (Bian et al., 2018; Jia et al., 2019). Total hardness (TH) ranged from 231.28 to 952.87 mg/L (average 465.42 mg/L) implying that 33.33% of the aquifer's water is hard, and other is very hard (Sawyer and McCarty, 1967). Water hardness has been linked to kidney disease and body tissue calcification (Dharmaratne, 2015; Dissanayake and Chandrajith, 2019) but no guideline for hardness has been developed (WHO, 2017).

Na^+ and K^+ ranged from 26.50 to 200.31 mg/L (average 96.53 mg/L) and 0.88–1.89 mg/L (average 1.51 mg/L) respectively. One sample representing 16.67% of the N aquifer's water exceeds the 200 mg/L drinking standard (WHO, 2017), while no drinking guideline has been set for K^+. The groundwater concentration of Ca^{2+} and Mg^{2+} in this aquifer all occur within recommended limits. Ca^{2+} ranges from 23.11 to 45.92 mg/L (average 33.07 mg/L), while Mg^{2+} varies from 9.17 to 29.99 mg/L (average 15.52 mg/L). Elevated Fe concentrations were observed in this aquifer with 83.33% of the samples exceeded national guidelines values of 0.3 mg/L (National Standardization Administration, 2017). Concentration ranged from 0.03 to 1.5 mg/L (average 0.74 mg/L). Fe is not often regarded as a hazardous groundwater pollutant though it can influence water palatability (Emenike et al., 2018). With Mn, Fe has been associated with chronic intoxication, lung embolism, impotence, nerve damage, and parkinsonism (Zoni, 2007). Geogenic origin has been inferred for high Fe concentration in the Songnen plain (Adeyeye et al., 2020; Jia et al., 2018; Zhang et al., 2020). Among the anions, HCO_3^- and CO_3^{2-} concentrations ranged from 217.36 to 428.32 mg/L (average 307.71 mg/L) and <1.47–6.29 mg/L (average of 1.47 mg/L), respectively. There is no guideline value determined for CO_3^{2-} in drinking water (WHO, 2017), and all the samples fall within recommended limits for HCO_3^-. Groundwater bicarbonate often originates from the natural dissolution of silicate and carbonate rocks and runoff and irrigation sources (Alaya et al., 2014; Emenike et al., 2018; Rasool et al., 2016). The groundwater Cl^- ranged from 6.05 to 126.35 mg/L (average 40.76 mg/L), with all samples occurring within recommended limits. For SO_{2-4}, all samples also occurred within guideline limits for drinking water with a range of 12.10–93.00 mg/L (average 35.02 mg/L). NO_3^-N ranged from <0.40–2.25 mg/L (average 0.81 mg/L). None of the samples exceeded the recommended NO_3^-–N guideline.

Most of the groundwater in Q_1 is Na+K – HCO_3+CO_3 (50%) and Ca+Mg – HCO_3+ CO_3 (47.73%), while Ca+Mg–SO_4–Cl waters occur marginally with 2.27% of the samples (Fig. 2). The pH is slightly alkaline as in the tertiary aquifer occurring within recommended limits. pH ranged from 7.76 to 8.40 (average 8.06). TDS ranged from 331 to 2834 mg/L (average 826.28 mg/L). Most of the groundwater was fresh and 20.45% was brackish exceeding the recommended guidelines. Total hardness (TH) ranged from 61.77 to 860.34 mg/L (average 266.53 mg/L), indicating 2.27%, 20.46%, 47.73%, and 29.55% were soft, moderately soft, hard, and very hard, respectively. Na^+ and K^+ ranged from 19.97 to 287.45 mg/L (average 102.93 mg/L) and 0.63–2.42 mg/L (average 1.43 mg/L) respectively. Out of the forty–four samples analyzed for this aquifer, only two representing 4.55% of the water from the aquifer exceeds the recommended drinking standard for Na^+. Similarly, 4.55% of the samples analyzed for Ca^{2+} and Mg^{2+}, respectively, exceeded the recommended limits. Ca^{2+} ranged from 11.80 to 104.30 mg/L (average 47.49 mg/L), while Mg^{2+} varied from 7.85 to 133.40 mg/L (average 23.14 mg/L). 100% of the samples have Fe concentration above recommended national limits (National Standardization Administration, 2017) and ranged from 0.05 to 2.42 mg/L (average 0.45 mg/L). No sample exceeded the recommended limits in terms of bicarbonate (HCO_3^-). HCO_3^- and CO_{2-3} concentrations ranged from 189.23 to 910.34 mg/L (average 388.59 mg/L) and <2.52–31.4 mg/L (average of 3.78 mg/L) respectively. Cl^- ranged from 8.90 to 266.00 mg/L (average 42.29 mg/L) with all samples occurring within recommended limits. SO_{2-4} on the other hand, along with NO_3^-N had 2.27% of the samples exceeding guideline limits. SO_4^{2-} ranged from 3.26 to 266.00 mg/L (average 43.29 mg/L) while groundwater NO_3^-N had range and average of < 0.2–2.25 mg/L and 0.81 mg/L respectively.

The Q_3 (2001) is mainly composed Ca+Mg – HCO_3+ CO_3 (42.55%) and Na+K – HCO_3+CO_3 (40.42%) groundwater facies while Ca+Mg–SO_4–Cl and Na+K–SO_4–Cl waters occur marginally with 12.77% and 4.26% respectively. The groundwater pH is also marginally alkaline though occurring within recommended limits with a range and average of 7.72–8.35 and 8.01, respectively. TDS ranged from 320 to 2743 mg/L (average 916.51 mg/L), with 34.04% being brackish. TH ranged from 128.48 to 809.56 mg/L (average 324.42 mg/L). Consequently, 12.77%, 42.55%, and 44.68 were moderately soft, hard, and very hard, respectively. In the case of Na^+, 31.91% of the water from the aquifer exceeds the recommended drinking standard for Na^+ (WHO, 2017). Na^+ and K^+ ranged from 43.59 to 714.42 mg/L (average 171.64 mg/L) and 0.25 – 6.38 mg/L (average 1.16 mg/L) respectively. Ca^{2+} ranged from 20.49 to 245.00 mg/L (average 75.62 mg/L) while Mg^{2+} varied from 16.21 to 169.20 mg/L (average 57.34 mg/L). About 21.28% and 40.42% of groundwater exceeded the recommended limits for Ca^{2+} and Mg^{2+}, respectively. As observed in previous aquifers (N and Q_1), 93.62% of groundwater samples have Fe concentration above national limits (National Standardization Administration, 2017). Fe ranges from 0.003 to 4.81 mg/L (average 0.38 mg/L). HCO_3^- and CO_{2-3} concentrations ranged from 232.06 to 920.56 mg/L (average 507.92 mg/L) and < 2.52–37.73 mg/L (average 6.55 mg/L) respectively. Cl^- ranged from 24.91 to 211.00 mg/L (average 169.07 mg/L), with 17.02% of samples occurring above the recommended limits (WHO, 2017). SO_{2-4} ranged from 1.00 to 211.00 mg/L (average 40.53 mg/L) with all samples occurring within WHO (2017) limits. However, 46.81% of the samples had groundwater NO_3^-N exceeding the guideline limits. Natural nitrate is often less than 15 mg/L (Chen et al., 2016; Naderi et al., 2020). Nitrate pollution is a cardinal indicator of anthropogenic influence on groundwater (Adimalla and Qian, 2019; Maila et al., 2004). The phreatic nature of this aquifer makes anthropogenic influences likely. NO_3^-N had a range and an average of < 1–389.00 mg/L and 106.5 mg/L, respectively.

In Q_3 (2017), the dominant water characteristic of the order Na+K – HCO_3+CO_3 (59.26%) > Ca+Mg – HCO_3+ CO_3 (33.33%) > Ca+Mg–SO_4–Cl (7.41%). The pH range and average were respectively 7.40–8.30 and 7.78. TDS ranged from 215 to 2080 mg/L (average 754.04 mg/L). Most of the water occurred within WHO drinking guidelines except 18.52%, which were brackish. TH ranged from 67.80 to 1080.00 mg/L (average 273.40 mg/L), implying 3.70%, 18.52%, 48.15%, and 29.63% were soft, moderately soft, hard, and very hard, respectively. Na^+ and K^+ ranged from 11.50 to 572.00 mg/L (average 168.29 mg/L) and 0.58–13.60 mg/L (average 1.89 mg/L) respectively. Na^+ had 29.63% of the samples exceeding the recommended standard WHO (2017). Ca^{2+} ranged from 15.40 to 154.00 mg/L (average 54.56 mg/L) while Mg^{2+} varied from 5.62 to 182.00 mg/L (average 33.65 mg/L). 3.70% and 18.52% of the Ca^{2+} and Mg^{2+} samples, respectively exceeded the recommended guideline. Fe ranged from 0.005 to 3.78 mg/L (average 1.16 mg/L). The sample HCO_3^- concentrations ranged from 234.00 to 1270.00 mg/L (average 535.11 mg/L), with 7.4% exceeding guideline limits (WHO, 2017). The average concentration of CO_{2-3} was 2.00 mg/L. Cl^- ranged from 3.52 to 246.00 mg/L (average 70.82 mg/L), with all samples occurring within recommended limits. SO_{2-4} ranged from 4.68 to 270.00 mg/L (average 63.16 mg/L) with all but one sample (3.70%) occurring within guideline limits. The Q_3 (2017) had a lower NO_3^-N pollution compared to Q_3

(2001) with range and average of 0.01 – 43.80 mg/L and 4.44 mg/L respectively. The nitrate content in groundwater is naturally determined by the depth of waterlogging, soil and aquifer texture, organic matter content, and precipitation amount. Irrigation returns also contribute to groundwater nitrate (Currell et al., 2012). Agricultural practices in the area have been maintained, and the soil and aquifer texture is constant in both 2001 and 2017. The only exception is that in 2001, the study area was recorded to have had the lowest rainfall. Rainfall may be directly proportional to nitrate concentration in groundwater as infiltration transports nitrate from human activities to groundwater (Kawagoshi et al., 2019; Pociene and Pocius, 2005). However, higher precipitation might serve in diluting nitrate in groundwater (Wick et al., 2012). The scenario is plausible in the area as irrigation is done using groundwater. In a low rainfall time, undiluted irrigation return flow may lead to higher nitrate concentrations, as seen in 2001. Additionally, the effects of rainfall on groundwater in the Songnen plain is usually far greater in the fourth quarter when the 2017 samples were collected than in the second quarter when 2001 samples were collected respectively (Yu, 2016).

4.2. Fluoride in groundwater

The average fluoride content of groundwater in aquifers in the study area was of the order Q_3 (2017) > Q_3 (2001) > Q_1 > N (Fig. 2n). The N–aquifer was optimum as 100% of all the samples occurred within the 0.5–1.5 mg/L guideline range WHO (2017). F^- ranged from 0.56 to 0.95 mg/L (average 0.75 mg/L). In Q_1, however, fluoride pollution was observed, with 36.36% and 15.91% above and below the recommended guidelines respectively. F^-concentration ranged from 0.35 to 4.12 mg/L (average 1.41 mg/L). A similar scenario was observed in Q_3 (2001), in which 57.44% and 23.40% of the samples occurred above and below the recommended guideline limit respectively. The F^-concentration in Q_3 (2001) ranged from 0.23 to 5.43 mg/L (average 2.03 mg/L). Fluoride pollution in Q_3 aquifer is persistent on a temporal scale because, in 2017, 51.85% and 14.89% respectively had concentrations above the standard with F^-concentration ranging from 0.33 to 7.99 mg/L (average 2.09 mg/L). The spatial distribution of fluoride displays a general decrease from the southwestern portion of the study area to the northwest (Fig. 1). The mean fluoride concentrations obtained in the multi-layered N, Q_1, and Q_3 aquifers are slightly lower than those obtained by Xibei (2007) in the respective aquifers and Zhang et al. (2003) in the Q_3 aquifer in 1998. The widespread distribution of the fluoride in both the confined and phreatic groundwater suggests a non-point source of fluoride pollution in the area (Luo et al., 2018).

4.3. Correlation matrix and saturation indices

Pearson correlation was used to appraise the effects of other physicochemical parameters on fluoride in the respective aquifers as has been done elsewhere (Dhiman and Keshari, 2006; Rasool et al., 2015; Rezaei et al., 2017; Singaraja et al., 2018). Correlation was tagged as weak, moderate and strong based on $r < 0.3$, $0.3 < r < 0.7$, and $r > 0.7$ respectively (Emenike et al., 2018; Salifu et al., 2012).

In the N aquifer, at a significance level of $p > 0.05$, fluoride had a moderate positive correlation of 0.633, 0.524, 0.482, 0.424, and 0.370 with Na^+, K^+, HCO_3^-, CO_{2-3}, and Cl^- respectively, highlighting the importance of alkaline waters to fluoride dissolution and desorption (Reddy et al., 2010; Saxena and Ahmed, 2003) (Table S3, Supplementary Material). Fluoride had a strong negative correlation with Ca^{2+} ($r = –0.781$) and moderate negative correlation with TH, TDS and Fe_T ($r = –0.321$, –0.501 and –0.565 respectively). Fluoride generally shows a negative relationship with Ca^{2+} (Dhiman and Keshari, 2006; Fawell et al., 2006; H. Jia et al., 2019; Singaraja et al., 2018; Subba Rao et al., 2016) indicating the influence of fluorite solubility on dissolved fluoride because $pK_{fluorite} = 10^{-6}$ (Parkhurst. and Appelo, 1999). When $[Ca^{2+}][F^-]^2$ is less than $K_{fluorite}$, fluorite dissolution is favoured while $[Ca^{2+}][F^-]^2$ greater than $K_{fluorite}$ encourages fluorite precipitation and decreases fluoride in water (Liu et al., 2015; Wei et al., 2016). Variation of Fluoride and Ca^{2+} activity in this study shows four groups (Fig. 4a): 1) samples occurring to the right of line 1 indicate fluoride is from sources other than fluorite; 2) samples between line 2 and line 3 suggest the strong role of fluorite mineral dissolution (especially in the N aquifer); 3) samples between line 1 and line suggest the influence of mineral precipitation and/or cation exchange on fluoride concentration (Q_1 and Q_3 aquifers); 4) samples which occur above $K_{fluorite}$ indicative of fluorite precipitation which limits fluoride dissolution in some groundwater samples from Q_3 in 2017. Jia et al. (2020) noted that SI calculated by PHREEQC only gives information about which phases are at a given stage of saturation but do not prove whether dissolution or precipitation occurs. The N, Q_1, Q_3 (2001), and Q_3 (2017) aquifer are all saturated concerning calcite (Fig. 4b–e). There is, however, no significant correlation between fluoride and calcite SI, which may be an indication that fluorite was heterogeneously distributed in the aquifer sediments and is not a consistent contributor to groundwater fluoride (Wei et al., 2016). The N aquifer is an exception with a moderate negative correlation of −0.551 between fluoride and calcite SI (Table S3, Supplementary Material). This is related to the strong influence of fluorite dissolution in the aquifer. The mechanism of Na–HCO_3 water fluoride release by calcite precipitation is given by Eqs. (7) and (8).

$$CaF_2 + \quad Na_2CO_2 \rightarrow CaCO_3 + 2Na^+ + 2F^- \tag{7}$$

$$CaF_2 + \quad NAHCO_3 \rightarrow CaCO_3 + 2Na^+ + 2F^- + H_2O + CO_2 \tag{8}$$

In the Q_1 aquifer, fluoride had moderate positive correlation with Mg^{2+}, HCO_3^-, and Na^+ ($r = 0.611$, 0.561, and 0.394 respectively, $p < 0.01$), moderate positive correlation with Cl^-, and NO_3^{2-} ($r = 0.372$ and 0.332, $p < 0.05$ respectively) and moderate negative correlation with TH and TDS ($r = –0.425$ and –0.429, $p < 0.01$ respectively) (Table S4, Supplementary Data). The positive relationship of fluoride with Mg^{2+} may be due to other fluoride-bearing minerals (Manikandan et al., 2014; Yan et al., 2020), precluding dolomite because aquifer shows dolomite saturation (Fig. 4b). The positive fluoride versus Mg^{2+} correlation may also be due to the formation of MgF^+ complexes due to salt effect (Luo et al., 2018).

Fluoride in Q_3 (2001), had moderate positive correlation with HCO_3^- ($r = 0.494$, $p < 0.01$) and moderate negative correlation with Ca^{2+} and pH ($r = –0.355$ and –0.433, $p < 0.05$ respectively) (Table S5, supplementary data). The negative relationship of fluoride with pH has been observed in some studies (Chae et al., 2006; Viero et al., 2009). It shows the importance of fluoride dissolution over desorption of fluoride from the surface of clays as is common at alkaline pH where OH^- and F^- compete for adsorption sites (Su et al., 2015). In 2017, fluoride in the Q_3 had a moderate positive correlation with HCO_3^-, Mg^{2+}, TDS, Na^+ and NO_3^- ($r = 0.573$, 0.442, 0.438, 0.403 and 0.384 respectively, $p < 0.05$) (Table S6, Supplementary Data). The positive relationship of fluoride to TDS and NO_3^- is related to the phreatic nature of the aquifer and thus climatic and anthropogenic influences (Xiao et al., 2015). In general, groundwater from aquifers in the study area is saturated in calcite, dolomite, and aragonite but undersaturated with fluorite and gypsum. The scenario thus enhances the dissolution of fluorite mineral in groundwater (Banerjee, 2015; Singh et al., 2011; Yidana et al., 2012) (Fig. 4b–e).

4.4. Ionic ratios

Several ionic ratios were used to identify the principal factors affecting fluoride concentration in groundwater in the area. The plots of $[(Ca+Mg)-(HCO_3+SO_4)]$ against (Na+K)-Cl was used to identify the occurrence of cation exchange in the various aquifers. $(Ca+Mg)-(HCO_3+SO_4)$ represents the amount of Ca^{2+} and Mg^{2+} added or removed from the system apart from that contributed by gypsum, calcite, and dolomite, while (Na+K)-Cl represents Na^+ added or

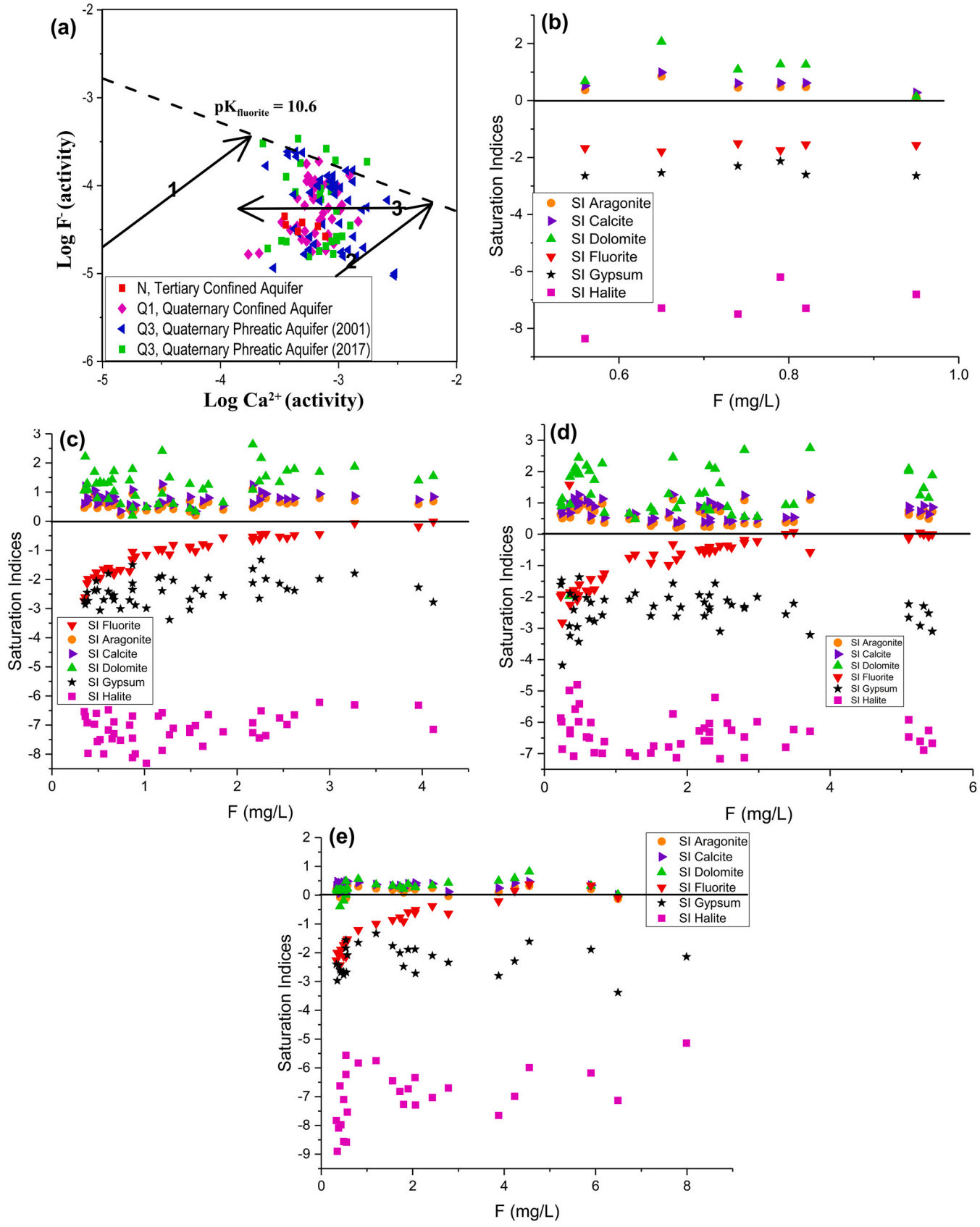

Fig. 4. (a) Relationship between the activities of Ca^{2+}_2 and F^-. Line 1 shows the path of fluorite dissolution; line 2 indicates the path of calcite and fluorite dissolution with a ratio of 200 (calcite/fluorite); line 3 shows that the path of Ca^{2+} decrease associated with calcite precipitation and/or cation exchange; and saturation indices of groundwater in various aquifers: (b) N, (c) Q_1, (d) Q_3 (2001), (e) Q_3 aquifer (2017).

removed from the system apart from chloride salts (mainly halite) (Jalali, 2007; Mondal et al., 2014). A linear relationship with a slope of −1 often implies the significant participation of Ca^{2+}, $Mg^{2+,}$ and Na^{+} ionic exchange within the system. Consequently, all the aquifers in the study area display a strong influence of cation exchange as the N, Q_1, Q_3 (2001), and Q_3 (2017) aquifers respectively had correlations of −0.941 (slope −0.576), −0.941 (slope −0.952), −0.935 (slope −0.882) and −0.931 (slope −0.805) (Fig. 5a). The cation exchange's importance was

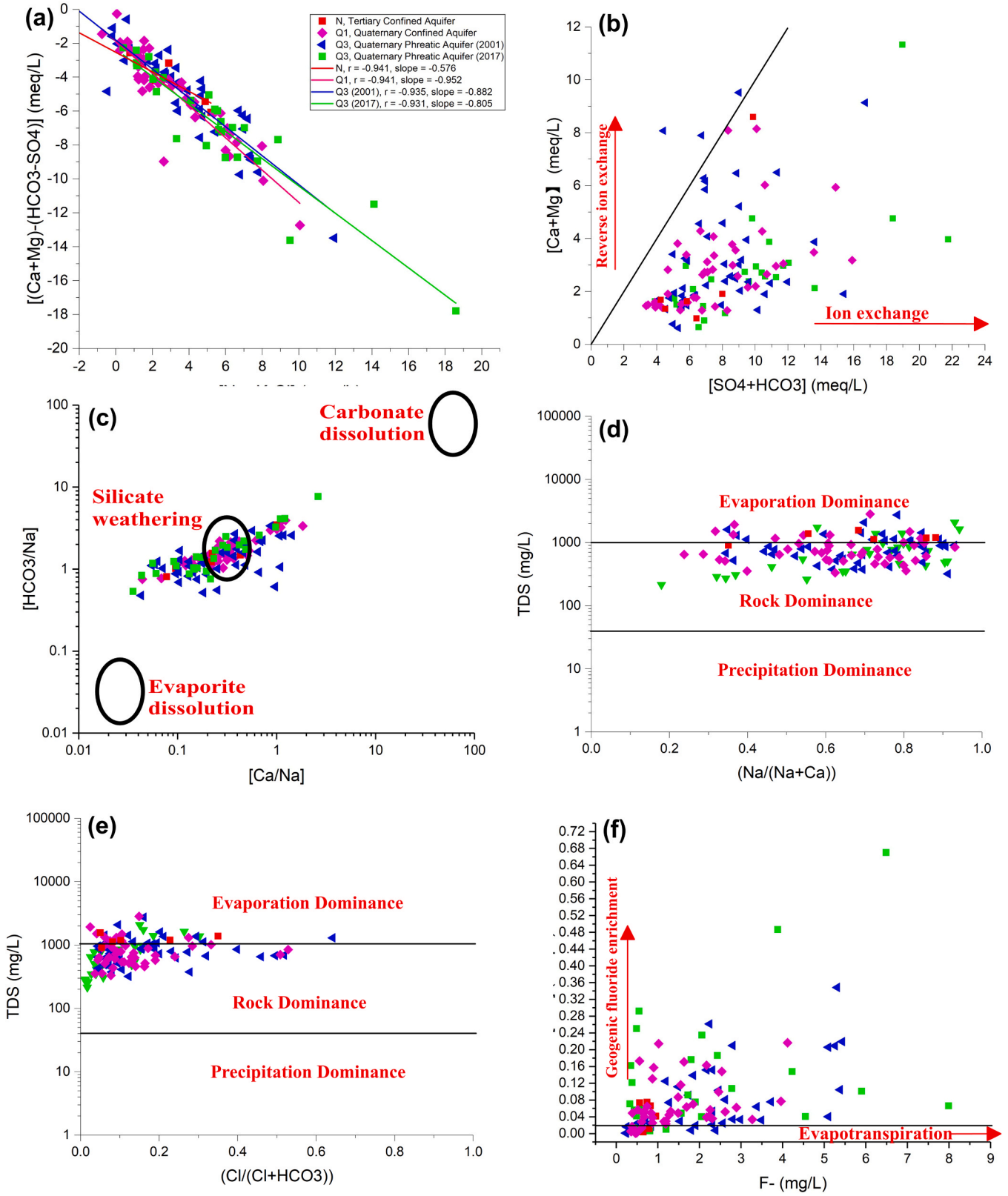

Fig. 5. Ionic scatter plots, (a) [(Ca+Mg)-(HCO_3+SO_4)] vs (Na+K)-Cl, (b) Ca+Mg vs HCO_3+SO_4, (c) [HCO_3]/[Na] vs [Ca]/[Na] (d) Gibbs Plot of Log_{10}TDS vs Na/(Na+Ca), (e) Gibbs Plot of Log_{10}TDS vs Cl/(Cl+HCO_3), (f) [F/Cl] vs F.

further emphasized using the Ca+ Mg versus SO_4+HCO_3 plot after Rezaei et al. (2017) (Fig. 5b). The majority of the samples from the N, Q_1, Q_3 (2001), and Q_3 aquifer (2017) aquifers occurred below the 1:1 line (except three samples representing 11.11% of the Q_3 aquifer in 2017), indicating the impact of cation exchange and silicate weathering on water chemistry in the whole aquifer system (Atkinson, 2018; Chen et al., 2020; Datta and Tyagi, 1996; Kaur et al., 2017).

The Na normalized HCO_3^- versus Ca^{2+} molar plots of Gaillardet et al. (1999) similarly displayed silicate weathering as a principal process governing groundwater chemistry to further emphasize the role of silicate weathering in determining groundwater chemistry.

Alkaline waters favour the desorption of fluoride from fluoride-bearing minerals like biotite, muscovite, and fluorite (Xiao et al., 2015). These minerals are present in the recharge zones and margin of the confined aquifers. Fluoride dissolution by hydrolysis (weathering) of fluoride-bearing minerals is displayed by Eqs. (9) to (11). Banerjee (2015) and Kumar & Saxena (2011) found that, though mineral dissolution by hydrolysis and dissolution pulled by calcite precipitation can contribute to groundwater fluoride contamination, dissolution by hydrolysis is more efficient in releasing fluoride in groundwater.

$$KAl_2[AlSi_3O_{10}]F_2 + \quad OH^- \rightarrow KAl_2[AlSi_3O_{10}](OH)_2 + \quad 2F^- \tag{9}$$

$$KMg_3[Al_3Si_3O_{10}]F_2 + \quad 2OH^- \rightarrow KMg_3[Al_3Si_3O_{10}](OH)_2 + \quad 2F^- \tag{10}$$

$$CaF_2 + \quad 2OH^- \rightarrow Ca(OH)_2 + \quad 2F^- \tag{11}$$

The TDS versus Na/(Na+Ca) and Cl/(Cl+HCO_3) diagram of Gibbs (1970) similarly showed the dominance of water-rock interaction in the chemistry of the water in all the aquifers in the study area (Fig. 5d and e). Additionally, evaporation contribution to groundwater was also noticed as some samples from both confined and phreatic aquifers occurred in the evaporation dominance zone. The semi-arid climate of the study area agrees with evaporation contribution to phreatic groundwater as species, including fluoride, are concentrated in groundwater by evaporation (Brahman et al., 2013; Xiao et al., 2015; Yan et al., 2020). On the contrary, in the confined aquifers, the display of evaporative dominance traits in some samples with high TDS may be due to leakage from the phreatic water into the confined aquifer (Z. Su et al., 2020). Such leakages have been reported in the study area and other parts of northern China (Bian et al., 2018; Yan et al., 2020; Jia et al., 2019). Further evidence of geogenic enrichment and mild evaporative contribution to groundwater fluoride is shown by the F/Cl versus F plot of Currell et al. (2011). High F/Cl ratios in most samples imply fluoride enrichment independent of evapotranspiration (Fig. 5f).

4.5. Fluoride and groundwater evolution along flow path

The inverse hydrogeochemical modelling result of the Q_3 aquifer along flow paths A–C in 2001 and X–Z in 2017 is shown (Fig. 1, Table S7 Supplementary Data). In the recharge zone (A–B), Ca+Mg-HCO_3-CO_3 facies dominate and evaporation occurs. Fluorite, dolomite, and halite are precipitated while gypsum and calcite remain in the solution. Cation exchange also occurs with Na^{2+} (0.00625 mmol/L) desorbed into groundwater from the surface of rock and soil by Ca^{2+}. Na+K-HCO_3-CO_3 facies dominates the runoff and/or discharge area. As groundwater continues from B–C, evaporation persists with calcite and fluorite being precipitated while other minerals remain in solution. Cation exchange in this flow transect involves Na^+ adsorption and Ca^{2+} release into groundwater (0.00709 mmol/L). In general, along the flow path A–C, fluorite is precipitated from solution, and fluoride concentration decreases contrary to many studies elsewhere (Haji et al., 2018; Wang et al., 2018; J. Li et al., 2020) and in the inland basin where the study is located (Du et al., 2009; M. Li et al., 2019). However, the observation is plausible as a local variation to the regional trend because the area is about 1/11th part of the 41,140 km^2 inland basin west of Jilin province and 1/49th part of the 178,000 km^2 Songnen plain, which is reported to have alternating high and low fluoride areas (B. Zhang et al., 2007). Additionally, regional groundwater flow in the north China plain displayed many local fluoride decreases in the central plain and coastal area though the regional trend increased (J. Li et al., 2020). Consequently, local transects of regional groundwater flow can show decreased fluoride. The low fluoride observed in this flow path may have been due to fluorite re-precipitation as displayed by inverse model or possible inclusion of fluoride in concretions because of the significant negative correlation between F and pH (Table S5, Supplementary Material), which hampers fluoride desorption (Su et al., 2015).

In 2017, along flow part X – Y, calcite was precipitated in the recharge area, characterized by Na+K-HCO_3-CO_3 facies. Other minerals remain in solution as CO_2 is added to the system with weak cation exchange with Ca^{2+} replacing Na^+ in solution (0.00038 mol/L). As groundwater moves from Y–Z, calcite is precipitated along with dolomite and gypsum with stronger cation exchange where Ca^{2+} replaces Na^+ (0.00217 mmol/L). Overall, along the flow path X–Z, fluoride is enriched along with halite, as corroborated by the significant positive correlation of fluoride with SI of fluorite and halite, respectively (Table S6, supplementary material).

Natural recharge of the multi-aquifers in the study area is believed to be from precipitation (Yan et al., 2020), including groundwater from N aquifer which has been estimated to be from modern precipitation using tritium values (Yang, 2008). The water originates at the fringes of the basin outside the study area. Within the study area, the phreatic Q_3 aquifer and the confined Q_1 and N aquifers are believed to have minimal contact due to the confining layer's thickness (15–45 m). On-site measurement and correlation of water quality parameters via a long pumping process were used to confirm the multi-aquifers' connection (Local Chronicles Compilation Committee of Jilin Province, 1992). The increased fluoride in the confined aquifers in many cases is a result of anthropogenic activities demonstrated by poor drilling practices, which destroys the confining bed leading to an increased hydraulic connection between the Q_3, $Q_1$and N aquifers, respectively (Jia et al., 2019; M. Li et al., 2020). A significant positive relationship between Fluoride and NO_3^- in the Q_1 indicates possible human influence on groundwater chemistry.

The study area lies in the central area of the Songnen plain, and groundwater movement is very slow. Consequently, fluoride in groundwater is believed to be enriched by dissolution processes, cation exchange, desorption, and groundwater evaporation. Since the phreatic and confined aquifers in the study area originate from similar processes, the higher fluoride concentration in the phreatic aquifer may be related to its sediment composition and exposure to additional hydrogeochemical processes like evaporation. Pang (1991) confirmed shallow sediments to have the highest fluoride concentration in the study area.

4.6. Health risk assessment

The non-carcinogenic fluoride health risk through oral and dermal pathways associated with using groundwater from the multi-layered aquifer in the study area is summarized in Table 1. The total hazard quotient (THQ) is in the order infant > children > adult. The trend is similar to other parts of the world, including China (Emenike et al., 2018; Guissouma et al., 2017; Rahman et al., 2020; Zhang et al., 2017). Also, the hazard quotient due to the ingestion pathway (HQ_{oral}) far exceeds that due to dermal contact (HQ_{dermal}), implying groundwater ingestion is the most critical means of fluoride exposure in the study area.

The THQ for infants, children and adults in N aquifer ranges from 0.8788 to 1.4907 (mean 1.1795), 0.5438–0.9225 (mean 0.7299) and 0.1971–0.3343 (mean 0.2645) respectively. No health risk occurs for children and adults due to groundwater from this aquifer. However, 83.33% of infants are at risk. For the Q_1 aquifer, THQ ranges from 0.5492 to 6.4651 (mean 2.2158), 0.3399–4.008 (mean 1.3712), and 0.1232–1.4498 (mean 0.4969) corresponding to infants, children, and

Table 1
Summary of computed fluoride hazard quotients through oral and ingestion pathways in the multi-aquifer layers in the study area.

Aquifer	Statistical parameter	Hazard quotient (oral pathway)			Hazard quotient (dermal pathway)			Total hazard quotient		
		Infant	Children	Adult	Infant	Children	Adult	Infant	Children	Adult
Tertiary Confined Aquifer (n = 6)[a]	Min	0.8742	0.5405	0.1947	0.0046	0.0033	0.0023	0.8788	0.5438	0.1971
	Mean	1.1734	0.7255	0.2614	0.0062	0.0044	0.0031	1.1795	0.7299	0.2645
	Median	1.1942	0.7384	0.2660	0.0063	0.0044	0.0032	1.2004	0.7429	0.2692
	Max	1.4829	0.9170	0.3304	0.0078	0.0055	0.0039	1.4907	0.9225	0.3343
	No. HQ > 1 (% > 1)[b]	5 (83.33)	nil	nil	nil	nil	nil	5 (83.33)	nil	nil
Quaternary Confined Aquifer (n = 44)[a]	Min	0.5464	0.3378	0.1217	0.0029	0.0020	0.0014	0.5492	0.3399	0.1232
	Mean	2.2042	1.3630	0.4911	0.0116	0.0082	0.0058	2.2158	1.3712	0.4969
	Median	1.8264	1.1293	0.4069	0.0096	0.0068	0.0048	1.8360	1.1361	0.4117
	Max	6.4313	3.9768	1.4328	0.0338	0.0240	0.0170	6.4651	4.0008	1.4498
	No. HQ > 1 (% > 1)[b]	33 (75.00)	23 (52.27)	4 (9.09)	nil	nil	nil	33 (75.00)	23 (52.27)	4 (9.09)
Quaternary Phreatic Aquifer (2001) (n = 47)[a]	Min	0.3590	0.2220	0.0800	0.0019	0.0013	0.0010	0.3609	0.2233	0.0809
	Mean	3.1692	1.9597	0.7060	0.0167	0.0118	0.0084	3.1858	1.9715	0.7144
	Median	2.8878	1.7857	0.6434	0.0152	0.0108	0.0077	2.9030	1.7965	0.6510
	Max	8.4762	5.2413	1.8883	0.0445	0.0316	0.0225	8.5208	5.2729	1.9108
	No. HQ > 1 (% > 1)[b]	34 (72.34)	30 (63.83)	10 (21.28)	nil	nil	nil	34 (72.34)	30 (63.83)	10 (21.28)
Quaternary Phreatic Aquifer (2017) (n = 27)[a]	Min	0.5151	0.3185	0.1148	0.0027	0.0019	0.0014	0.5178	0.3205	0.1161
	Mean	3.9162	2.4216	0.8724	0.0206	0.0146	0.0104	3.9368	2.4362	0.8828
	Median	3.7932	2.3456	0.8451	0.0199	0.0141	0.0101	3.8132	2.3597	0.8551
	Max	12.4724	7.7124	2.7786	0.0655	0.0465	0.033	12.5379	7.7588	2.8116
	No. HQ > 1 (% > 1)[b]	16 (59.26)	15 (55.56)	6 (22.22)	nil	nil	nil	16 (59.26)	15 (55.56)	6 (22.22)

[a] Means the number of samples.
[b] means the number of samples with Health Quotient > 1 (percentage of samples with Health Quotient > 1).

adults, respectively. 75% of infants, 23% of children, and 9.09% of adults using groundwater from this aquifer are exposed to fluoride risk. A perusal of the spatial distribution THQ due to water from this aquifer reveals wells in the northern portion of the study area are safer than those in the south (Fig. 6a–c).

In the Q_3 aquifer in the year 2001, THQ ranges from 0.3609 to 8.5208 (mean 3.1858) in infants, 0.2233–5.2729 (mean 1.9715) in children, and 0.0809–1.9108 (mean 0.7144) in adults. The results indicate that 72% of infants, 63% of children, and 21.28% of adults are liable to non-carcinogenic health risks using water from the aquifer. The data displays a spatial increase in health risk from north to south (Fig. 6d–f). In 2017, THQ for infants, children and adults respectively ranges from 0.5178 to 12.5379 (mean 3.93), 0.3205–7.7588 (mean 2.4362) and 0.1161–2.8116 (mean 0.8828). Conversely, using water from this aquifer in 2017 exposes 59% of infants, 55.56% of children, and 22.22% of adults to health risks. Although the percentage exposure to fluoride risk in the Q_3 aquifer shows a marginal decrease between 2001 and 2017 as has been observed elsewhere in China (Y. Li et al., 2019), the mean THQ of the respective aquifer layers is of the order $Q_3(2017) > Q_3\ (2001) > Q_1 > N$. Thus, though deeper confined aquifers N and Q_1 have better groundwater quality compared to the phreatic aquifer in the study area, there is still considerable non-carcinogenic health risk such as dental fluorosis, skeletal fluorosis, crippling fluorosis and detrimental effects on the kidneys associated the use (Demelash et al., 2019; Dharmaratne, 2019; Dissanayake and Chandrajith, 2019; Malago, 2017).

5. Conclusion

The groundwater fluoride hydrochemistry of multiple aquifer layers was studied to determine the non-carcinogenic health risks associated with groundwater from the respective layers. The following conclusions were drawn:

1. Groundwater pH in the area was slightly alkaline, ranging from 7.40 in Q_3 (2017) to 8.45 in N. The dominant water type was $Na+K–HCO_3+CO_3$ in all aquifers except Q_1, where $Ca+Mg – HCO_3$ CO_3 water facies was marginally dominant.
2. Fluoride concentrations below and/or above the recommended guideline occurred in all the aquifers except N, where concentrations were optimum in all samples analyzed. The mean fluoride concentration of groundwater in the aquifers was of the order Q_3 (2017) > Q_3 (2001) > Q_1> N with 51.85%, 57.44%, 36.36% and 0% occurring below/above recommended guideline values respectively.
3. Silicate weathering, cation exchange, and fluorite dissolution determined fluoride concentration in groundwater. Evaporation contributed to fluoride concentration in the Q_3 aquifer by forming $MgF+$ complexes in Q_1 and Q_3 (2017), respectively.
4. Computed THQ from both oral and dermal pathways show risks of the order infant > children > adult. The associated risks liable from using water in the respective aquifer layers is of the order Q_3 (2017) > Q_3 (2001) > Q_1> N.
5. The mean groundwater fluoride in 2017 was marginally higher than that of 2001 (2.09>2.03 mg/L respectively), although the percentage of age group members disposed to fluoride risk from using water from Q_3 decreased from 2001 to 2017.

Though the deeper confined aquifers are better quality than the phreatic aquifers in fluoride pollution, considerable health risk still exists in using some deep confined aquifers like Q_1. Therefore knowledge of local hydrogeology in exploiting deep groundwater free of fluoride pollution and on-site defluoridation treatment of groundwater is recommended for the study area and other areas with similar characteristics.

Funding

This study is supported by the National Natural Science Foundation of China (41572216), the China Geological Survey Shenyang Center "Hydrogeological Survey of Songnen Plain" project (DD20190340-W09), the Geological Survey Foundation of Jilin Province (2018–13), and Petroleum Technology Development Fund (PTDF) Nigeria (PTDF/ED/PHD/OPA/61/18).

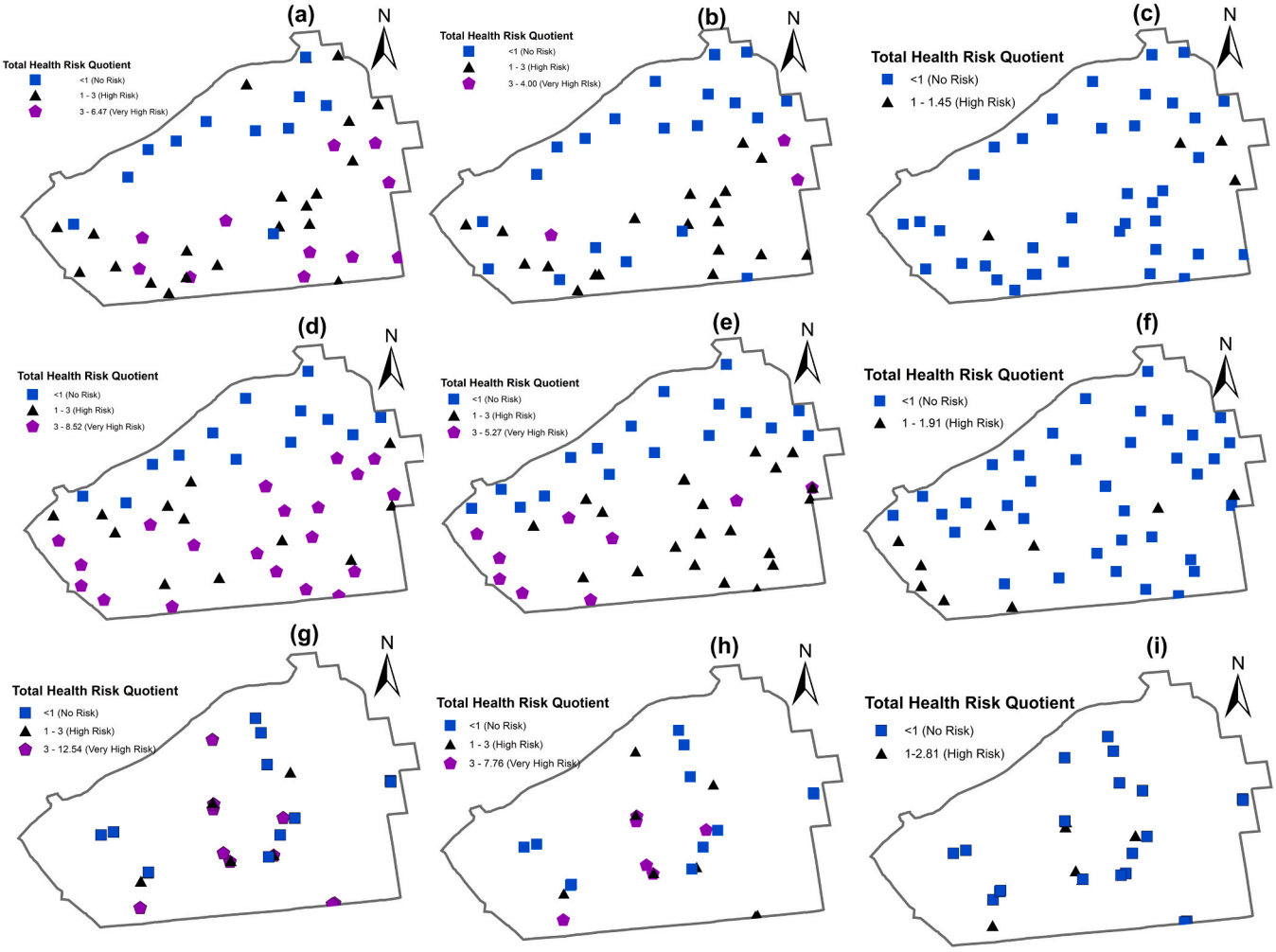

Fig. 6. Symbol map showing the spatial distribution of total hazard quotient (THQ) of (a) infants in Q_1, (b) children in Q_1, (c) adults in Q_1, (d) infants in Q_3 (2001), (e) children in Q_3 (2001), (f) adults in Q_3 (2001), (g) infants in Q_3 (2017), (h) children in Q_3 (2001), (i) adults in Q_3 (2017).

CRediT authorship contribution statement

Oluwafemi Adewole Adeyeye: Conceptualization, Data curation, Formal analysis, Funding acquisition, Investigation, Methodology, Software, Validation, Visualization. **Changlai Xiao:** Conceptualization, Funding acquisition, Investigation, Methodology, Project adminiistration, Resources, Supervision, Validation. **Zhihao Zhang:** Data curation, Formal analysis, Investigation, Methodology, Validation, Visualization. **Achivir Stella Yawe:** Data curation, Formal analysis, Validation. **Xiujuan Liang:** Funding acquisition, Investigation, Methodology, Project administration, Resources, Supervision, Validation.

Declaration of Competing Interest

The authors declare that they have no known competing financial interests or personal relationships that could have appeared to influence the work reported in this paper.

Acknowledgments

Authors are grateful to Jingyu Field Base for Volcanoes and Mineral Springs, Jilin Province for their support in carrying out this research. The two anonymous reviewers are also appreciated for their contribution in improving the quality of the manuscript.

Appendix A. Supporting information

Supplementary data associated with this article can be found in the online version at doi:10.1016/j.ecoenv.2021.111926.

References

Adeyeye, O., Xiao, C., Zhang, Z., Liang, X., 2020. State, source and triggering mechanism of iron and manganese pollution in groundwater of Changchun, Northeastern China. Environ. Monit. Assess. 192 (10), 1–15. https://doi.org/10.1007/s10661-020-08571-0.

Adimalla, N., Qian, H., 2019. Groundwater quality evaluation using water quality index (WQI) for drinking purposes and human health risk (HHR) assessment in an agricultural region of Nanganur, south India. Ecotoxicol. Environ. Saf. 176 (126), 153–161. https://doi.org/10.1016/j.ecoenv.2019.03.066.

Alaya, M.B., Saidi, S., Zemni, T., Zargouni, F., 2014. Suitability assessment of deep groundwater for drinking and irrigation use in the Djefara aquifers (Northern Gabes, south-eastern Tunisia). Environ. Earth Sci. 71, 3387–3421.

Amini, H., Ali, G., Masud, H., Ramin, Y., 2016. Spatial and temporal variability of fluoride concentrations in groundwater resources of Larestan and Gerash regions in Iran from 2003 to 2010. Environ. Geochem. Health 38, 25–37. https://doi.org/10.1007/s10653-015-9676-1.

Apambire, W.B., Boyle, D.R., Michel, F.A., 1997. Geochemistry, genesis, and health implications of fluoriferous groundwaters in the upper regions of Ghana. Environ. Geol. 33 (1), 13–24. https://doi.org/10.1007/s002540050221.

Atkinson, J.C., 2018. Evaluation and interpretation of historical major-ion chemistry for the Lodgepole Creek Watershed, Nebraska. Environ. Earth Sci. 77 (3), 55. https://doi.org/10.1007/s12665-017-7202-8.

Ayoob, S., Gupta, A.K., 2006. Fluoride in drinking water: a review on the status and stress effects. Crit. Rev. Environ. Sci. Technol. 36 (6), 433–487. https://doi.org/10.1080/10643380600678112.

Banerjee, A., 2015. Groundwater fluoride contamination: a reappraisal. Geosci. Front. 6 (2), 277–284. https://doi.org/10.1016/j.gsf.2014.03.003.
Bian, J., Nie, S., Wang, R., Wan, H., Liu, C., 2018. Hydrochemical characteristics and quality assessment of groundwater for irrigation use in central and eastern Songnen Plain, Northeast China. Environ. Monit. Assess. 190 (7), 382. https://doi.org/10.1007/s10661-018-6774-4.
Brahman, K.D., Kazi, T.G., Afridi, H.I., Naseem, S., Arain, S.S., Wadhwa, S.K., Shah, F., 2013. Simultaneously evaluate the toxic levels of fluoride and arsenic species in underground water of Tharparkar and possible contaminant sources: a multivariate study. Ecotoxicol. Environ. Saf. 89, 95–107. https://doi.org/10.1016/j.ecoenv.2012.11.023.
Chae, G.T., Yun, S.T., Kwon, M.J., Kim, S.Y., Mayer, B., 2006. Batch dissolution of granite and biotite in water: implication for fluorine geochemistry in groundwater. Geochem. J. 40, 95–102. https://doi.org/10.2343/geochemj.40.95.
Chen, J., Qian, H., Wu, H., 2017. Nitrogen contamination in groundwater in an agricultural region along the New Silk Road, northwest China: distribution and factors controlling its fate. Environ. Sci. Pollut. Res. 24 (15), 13154–13167. https://doi.org/10.1007/s11356-017-8881-0.
Chen, J., Wu, H., Qian, H., 2016. Groundwater nitrate contamination and associated health risk for the rural communities in an agricultural area of Ningxia, northwest China. Expo. Heal 8, 349–359.
Chen, Q., Jia, C., Wei, J., Dong, F., Yang, W., Hao, D., Jia, Z., Ji, Y., 2020. Geochemical process of groundwater fluoride evolution along global coastal plains: Evidence from the comparison in seawater intrusion area and soil salinization area. Chemical Geology 555, 119779. https://doi.org/10.1016/j.chemgeo.2020.119779.
Currell, M., Cartwright, I., Raveggi, M., Han, D., 2011. Controls on elevated fluoride and arsenic concentrations in groundwater from the Yuncheng Basin, China. Appl. Geochem. 26 (4), 540–552. https://doi.org/10.1016/j.apgeochem.2011.01.012.
Currell, M.J., Dongmei Han, Z.C., I. C, 2012. Sustainability of groundwater usage in northern China: dependence on palaeowaters and effects on water quality, quantity and ecosystem health. Hydrol. Process. 26, 4050–4066. https://doi.org/10.1002/hyp.9208.
Datta, P.S., Tyagi, S.K., 1996. Major ion chemistry of groundwater in Delhi area: chemical weathering processes and groundwater flow regime. J. Geol. Soc. India 47, 179–188.
Demelash, H., Beyene, A., Abebe, Z., Melese, A., 2019. Fluoride concentration in groundwater and prevalence of dental fluorosis in Ethiopian Rift Valley: systematic review and meta-analysis. BMC Public Health 19 (1), 1–9. https://doi.org/10.1186/s12889-019-7646-8.
Dharmaratne, R.W., 2015. Fluoride in drinking water and diet: the causative factor of chronic kidney diseases in the North Central Province of Sri Lanka. Environ. Health Prev. Med. 20 (4), 237–242.
Dharmaratne, R.W., 2019. Exploring the role of excess fluoride in chronic kidney disease: a review. Hum. Exp. Toxicol. 38 (3), 269–279. https://doi.org/10.1177/0960327118814161.
Dhiman, S.D., Keshari, A.K., 2006. Hydrogeochemical evaluation of high-fluoride groundwater: a case study from Mehsana District, Gujarat, India. Hydrol. Sci. J. 51 (6), 1149–1162. https://doi.org/10.1623/hysj.51.6.1149.
Dissanayake, C.B., Chandrajith, R., 2019. Fluoride and hardness in groundwater of tropical regions – review of recent evidence indicating tissue calcification and calcium phosphate nanoparticle formation in kidney tubules. Ceylon J. Sci. 48 (3), 197. https://doi.org/10.4038/cjs.v48i3.7643.
Du, C., Xiao, C., Feng, B., Liang, X., Zhe Ma, D.Z., 2009. Research on inverse geochemical simulation of phreatic water in western Jilin Province. In: C. Z., Tang, H. (Eds.), Advances in Water Resources and Hydraulic Engineering Proceedings of 16th IAHR-APD Congress and 3rd Symposium of IAHR-ISHS, ed.,. Tsinghua University Press, pp. 205–208.
Emenike, C.P.G., Tenebe, I.T., Jarvis, P., 2018. Fluoride contamination in groundwater sources in Southwestern Nigeria: assessment using multivariate statistical approach and human health risk. Ecotoxicol. Environ. Saf. 156, 391–402. https://doi.org/10.1016/j.ecoenv.2018.03.022.
Farooqi, A., Masuda, H., Firdous, N., 2007. Toxic fluoride and arsenic-contaminated groundwater in the Lahore and Kasur districts, Punjab, Pakistan and possible contaminant sources. Environ. Pollut. 145 (3), 839–849. https://doi.org/10.1016/j.envpol.2006.05.007.
Fawell, J., Bailey, K., Chilton, J., Dahi, E., Fewtrell, L., Magara, Y., 2006. Fluoride in drinking water. In: Community Dentistry and Oral Epidemiology, Vol. 8. World Health Organization and IWA Publishing,. https://doi.org/10.1111/j.1600-0528.1980.tb01289.x.
Gaillardet, J., Dupre, B., Louvat, P., A. C. J, 1999. Global silicate weathering and CO_2 consumption rates deduced from the chemistry of large rivers. Chem. Geol. 159 (1), 3–30.
Gazzano, E., Bergandi, L., Riganti, C., Aldieri, E., Doublier, S., Costamagna, C., Bosia, A., Ghigo, D., 2010. Fluoride effects: the two faces of janus. Curr. Med. Chem. 17 (22), 2431–2441. https://doi.org/10.2174/092986710791698503.
Gibbs, R.J., 1970. Mechanisms controlling world water chemistry. Science 170 (3962), 1088–1090. https://doi.org/10.1126/science.170.3962.1088.
Goldberg, M., 2018. Fluoride: double-edged sword implicated in caries prevention and in fluorosis. J. Cell Dev. Biol. 1 (1), 10–22.
Guissouma, W., Hakami, O., Al-Rajab, A.J., Tarhouni, J., 2017. Risk assessment of fluoride exposure in drinking water of Tunisia. Chemosphere 177, 102–108. https://doi.org/10.1016/j.chemosphere.2017.03.011.
Haji, M., Wang, D., Li, L., Qin, D., Guo, Y., 2018. Geochemical evolution of fluoride and implication for F- enrichment in groundwater: example from the Bilate River Basin of Southern Main Ethiopian Rift. Water (Switzerland) 10 (12), 1–20. https://doi.org/10.3390/w10121799.
Jalali, M., 2007. Hydrochemical identification of groundwater resources and their changes under the impacts of human activity in the Chah basin in western Iran. Environ. Monit. Assess. 130 (1–3), 347–364. https://doi.org/10.1007/s10661-006-9402-7.
Jia, H., Qian, H., Qu, W., Zheng, L., Feng, W., Ren, W., 2019. Fluoride occurrence and human health risk in drinking water wells from southern edge of Chinese loess plateau. Int. J. Environ. Res. Public Health 16 (10), 1683. https://doi.org/10.3390/ijerph16101683.
Jia, H., Qian, H., Zheng, L., Feng, W., Wang, H., Gao, Y., 2020. Alterations to groundwater chemistry due to modern water transfer for irrigation over decades. Sci. Total Environ. 717 (126), 137170 https://doi.org/10.1016/j.scitotenv.2020.137170.
Jia, Y., Xi, B., Jiang, Y., Guo, H., Yang, Y., Lian, X., Han, S., 2018. Distribution, formation and human-induced evolution of geogenic contaminated groundwater in China: a review. Sci. Total Environ. 643, 967–993. https://doi.org/10.1016/j.scitotenv.2018.06.201.
Kaur, T., Bhardwaj, R., Arora, S., 2017. Assessment of groundwater quality for drinking and irrigation purposes using hydrochemical studies in Malwa region, southwestern part of Punjab, India. Appl. Water Sci. 7 (6), 3301–3316. https://doi.org/10.1007/s13201-016-0476-2.
Kawagoshi, Y., Suenaga, Y., Chi, N.L., Hama, T., Ito, H., Duc, L. Van, 2019. Understanding nitrate contamination based on the relationship between changes in groundwater levels and changes in water quality with precipitation fluctuations. Sci. Total Environ. 657, 146–153. https://doi.org/10.1016/j.scitotenv.2018.12.041.
Kumar, S., Saxena, A., 2011. Chemical weathering of the Indo-Gangetic Alluvium with special reference to release of fluoride in the groundwater, Unnao district, Uttar Pradesh. J. Geol. Soc. India 77, 459–477.
Liao, Z.S., Lin, X.Y., 2004. Chemical characteristics and variations of groundwater quality in Songnen Basin. Earth Sci. 29 (1), 96–102.
Liu, H., Guo, H., Yang, L., Wu, L., Li, F., Li, S., Ni, P., Liang, X., 2015. Occurrence and formation of high fluoride groundwater in the Hengshui area of the North China Plain. Environ. Earth Sci. 74 (3), 2329–2340. https://doi.org/10.1007/s12665-015-4225-x.
Li, M., Liang, X., Xiao, C., Cao, Y., Hu, S., 2019a. Hadrochemical evolution of groundwater in a typical semi-arid groundwater storage basin using a zoning model. Water (Switzerland) 11 (7). https://doi.org/10.3390/w11071334.
Li, Y., Wang, F., Feng, J., Lv, J.p., Liu, Q., Nan, F.R., Zhang, W., Qu, W.y., Xie, S.L., 2019b. Long term spatial-temporal dynamics of fluoride in sources of drinking water and associated health risks in a semi-arid region of Northern China. Ecotoxicol. Environ. Saf. 171, 274–280. https://doi.org/10.1016/j.ecoenv.2018.12.090.
Li, J., Wang, Y., Zhu, C., Xue, X., Qian, K., Xie, X., Wang, Y., 2020a. Hydrogeochemical processes controlling the mobilization and enrichment of fluoride in groundwater of the North China Plain. Sci. Total Environ. 730, 138877 https://doi.org/10.1016/j.scitotenv.2020.138877.
Li, M., Xiao, C., Liang, X., Cao, Y., Hu, S., 2020b. Hydrogeochemical evolution under a changing environment: a case study in Jilin, China. Water Supply 1–11. https://doi.org/10.2166/ws.2020.072.
Local Chronicles Compilation Committee of Jilin Province, 1992. Chronicles of Jilin Province the Fourth Volume: Physical Geography, 4th ed.,. Jilin People's Publishing House.
Luo, W., Gao, X., Zhang, X., 2018. Geochemical processes controlling the groundwater chemistry and fluoride contamination in the yuncheng basin, China—an area with complex hydrogeochemical conditions. PLoS One 13 (7), 1–25. https://doi.org/10.1371/journal.pone.0199082.
Maila, Y.A., EI-Nahal, I., Al-Agha, M.R., 2004. Seasonal variations and mechanisms of groundwater nitrate pollution in the Gaza Strip. Environ. Geol. 47, 84–90.
Malago, J., 2017. Fluoride levels in surface and groundwater in Africa: a review. Am. J. Water Sci. Eng. 3 (1), 1. https://doi.org/10.11648/j.ajwse.20170301.11.
Manikandan, S., Chidambaram, S., Ramanathan, A.L., Prasanna, M.V., Karmegam, U., Singaraja, C., Paramaguru, P., Jainab, I., 2014. A study on the high fluoride concentration in the magnesium-rich waters of hard rock aquifer in Krishnagiri district, Tamilnadu, India. Arab. J. Geosci. 7 (1), 273–285. https://doi.org/10.1007/s12517-012-0752-x.
Mondal, D., Gupta, S., Reddy, D.V., Nagabhushanam, P., 2014. Geochemical controls on fluoride concentrations in groundwater from alluvial aquifers of the Birbhum district, West Bengal, India. J. Geochem. Explor. 145, 190–206.
Mukherjee, I., Singh, U.K., 2018. Groundwater fluoride contamination, probable release, and containment mechanisms: a review on Indian context. In: Environmental Geochemistry and Health, Vol. 40. Springer Netherlands,. https://doi.org/10.1007/s10653-018-0096-x.
Naderi, M., Jahanshahi, R., Dehbandi, R., 2020. Two distinct mechanisms of fluoride enrichment and associated health risk in springs' water near an inactive volcano, southeast Iran. Ecotoxicol. Environ. Saf. 195, 110503 https://doi.org/10.1016/j.ecoenv.2020.110503.
National Standardization Administration. (2017). Standard for groundwater quality.
NEPS-PRC. (2009). Technical requirements for water quality sampling scheme design, HJ495.
Pang, J., 1991. Preliminary study on the distribution and causes of shallow high fluorine groundwater in Qian'an County. Jilin Geol. 1 (1), 71–74.
Parkhurst, D.L. and Appelo, C.A.J. (1999). User's Guide to PHREEQC (Version - 2) - A Computer Program for Speciation, Batch-Reactions, One-Dimensional Transport, and Inverse Geochemical Calculations. Water-Resouces Investigation Report 99-4259. U. S. Geological Survey.
Piper, A.M., 1944. A graphic procedure in the geochemical interpretation of water-analyses. Eos Trans. Am. Geophys. Union 25, 914–928. https://doi.org/10.1029/TR025i006p00914.

Pociene, A., Pocius, S., 2005. Relationship between nitrate amount in groundwater and natural factors. J. Environ. Eng. Landsc. Manag. 13 (1), 23–30. https://doi.org/10.1080/16486897.2005.9636842.
Qian, H., Chen, J., Howard, K.W.F., 2020. Assessing groundwater pollution and potential remediation processes in a multi-layer aquifer system. Environ. Pollut. 263, 114669 https://doi.org/10.1016/j.envpol.2020.114669.
Rahman, M.M., Bodrud-Doza, M., Siddiqua, M.T., Zahid, A., Islam, A.R.M.T., 2020. Spatiotemporal distribution of fluoride in drinking water and associated probabilistic human health risk appraisal in the coastal region, Bangladesh. Sci. Total Environ. 724. https://doi.org/10.1016/j.scitotenv.2020.138316.
Rasool, A., Xiao, T., Baig, Z.T., Masood, S., Mostofa, K.M.G., Iqbal, M., 2015. Co-occurrence of arsenic and fluoride in the groundwater of Punjab, Pakistan: source discrimination and health risk assessment. Environ. Sci. Pollut. Res. 22 (24), 19729–19746. https://doi.org/10.1007/s11356-015-5159-2.
Rasool, A., Xiao, T., Farooqi, A., Shafeeque, M., Masood, S., Ali, S., Fahad, S., Nasim, W., 2016. Arsenic and heavy metal contaminations in the tube well water of Punjab, Pakistan and risk assessment: a case study. Ecol. Eng. 95, 90–100. https://doi.org/10.1016/j.ecoleng.2016.06.034.
Reddy, D.V., Nagabhushanam, P., Sukhija, B.S., Reddy, A.G.S.S., Smedley, P.L., 2010. Fluoride dynamics in the granitic aquifer of the Wailapally watershed, Nalgonda District, India. Chem. Geol. 269 (3–4), 278–289. https://doi.org/10.1016/j.chemgeo.2009.10.003.
Rezaei, M., Nikbakht, M., Shakeri, A., 2017. Geochemistry and sources of fluoride and nitrate contamination of groundwater in Lar area, south Iran. Environ. Sci. Pollut. Res. 24 (18), 15471–15487. https://doi.org/10.1007/s11356-017-9108-0.
Salifu, A., Petrusevski, B., Ghebremichael, K., Buamah, R., Amy, G., 2012. Multivariate statistical analysis for fluoride occurrence in groundwater in the Northern region of Ghana. J. Contam. Hydrol. 140–141, 34–44. https://doi.org/10.1016/j.jconhyd.2012.08.002.
Sawyer, C.N., McCarty, P.L., 1967. Chemistry for Sanitary Engineers (second). McGraw-Hill,.
Saxena, V., Ahmed, S., 2003. Inferring the chemical parameters for the dissolution of fluoride in groundwater. Environ. Geol. 43 (6), 731–736. https://doi.org/10.1007/s00254-002-0672-2.
Singaraja, C., Chidambaram, S., Jacob, N., Johnson Babu, G., Selvam, S., Anandhan, P., Rajeevkumar, E., Balamurugan, K., Tamizharasan, K., 2018. Origin of high fluoride in groundwater of the Tuticorin district, Tamil Nadu, India. Appl. Water Sci. 8 (2), 1–14. https://doi.org/10.1007/s13201-018-0694-x.
Singh, C.K., Rina, K., Singh, R.P., Shashtri, S., Kamal, V., Mukherjee, S., 2011. Geochemical modeling of high fluoride concentration in groundwater of Pokhran area of Rajasthan, India. Bull. Environ. Contam. Toxicol. 86 (2), 152–158. https://doi.org/10.1007/s00128-011-0192-4.
Subba Rao, N., Dinakar, A., Surya Rao, P., Rao, P.N., Madhnure, P., Prasad, K.M., Sudarshan, G., 2016. Geochemical processes controlling fluoride-bearing groundwater in the granitic aquifer of a semi-arid region. J. Geol. Soc. India 88 (3), 350–356. https://doi.org/10.1007/s12594-016-0497-3.
Su, C., Wang, Y., Xie, X., Zhu, Y., 2015. An isotope hydrochemical approach to understand fluoride release into groundwaters of the Datong Basin, Northern China. Environ. Sci. Process. Impacts 17 (4), 791–801. https://doi.org/10.1039/c4em00584h.
Su, Z., Wu, J., He, X., Elumalai, V., 2020. Temporal changes of groundwater quality within the groundwater depression cone and prediction of confined groundwater salinity using grey Markov model in Yinchuan Area of Northwest China. Expo. Health 12 (3), 447–468. https://doi.org/10.1007/s12403-020-00355-8.
US EPA, 1989. Risk Assessment Guidance for Superfund Volume I Human Health Evaluation Manual (Part A). https://doi.org/https://doi.org/EPA/540/1–89/002.
Viero, A.P., Roisenberg, C., Roisenberg, A., Vigo, A., 2009. The origin of fluoride in the granitic aquifer of Porto Alegre, Southern Brazil. Environ. Geol. 56 (8), 1707–1719. https://doi.org/10.1007/s00254-008-1273-5.
Wang, Y., Deng, C., Liu, Y., Niu, Z., Li, Y., 2018. Identifying change in spatial accumulation of soil salinity in an inland river watershed, China. Sci. Total Environ. 621, 177–185. https://doi.org/10.1016/j.scitotenv.2017.11.222.
Wang, H., He, H., Wang, H., Zhou, Z., Yu, C., 2019. Trends of fluoride control in China. Environ. Earth Sci. 78 (19), 1–8. https://doi.org/10.1007/s12665-019-8576-6.
Wang, W., Li, R., Tan, J., Luo, K., Yang, L., Li, H., Li, Y., 2002. Adsorption and leaching of fluoride in soils of China. Fluoride 35 (2), 122–129.
Wei, C., Guo, H., Zhang, D., Wu, Y., Han, S., An, Y., Zhang, F., 2016. Occurrence and hydrogeochemical characteristics of high-fluoride groundwater in Xiji County, southern part of Ningxia Province, China. Environ. Geochem. Health 38 (1), 275–290. https://doi.org/10.1007/s10653-015-9716-x.
Wen, D., Zhang, F., Zhang, E., Wang, C., Han, S., Zheng, Y., 2013. Arsenic, fluoride and iodine in groundwater of China. J. Geochem. Explor. 135, 1–21. https://doi.org/10.1016/j.gexplo.2013.10.012.
WHO. (2017). Guidelines for Drinking-Water Quality: fourth edition incorporating the first addendum (fourth). World Health Organization.
Wick, K., Heumesser, C., Schmid, E., 2012. Groundwater nitrate contamination: Factors and indicators. J. Environ. Manag. 111, 178–186. https://doi.org/10.1016/j.jenvman.2012.06.030.
Xiao, J., Jin, Z., Zhang, F., 2015. Geochemical controls on fluoride concentrations in natural waters from the middle Loess Plateau, China. J. Geochem. Explor. 159, 252–261. https://doi.org/10.1016/j.gexplo.2015.09.018.
Xibei, S., 2007. Distribution and Origin of Fluoride in Water and Soil Environment and the Ecological Effects in Jilin Qian'an. Jilin University.
Yang, X.K., 2008. Estimation of Groundwater Recharge and Renewal Rate Based on Environmental Isotopes in Songyuan Plain. China University of Geosciences.
Yan, J., Chen, J., Zhang, W., Ma, F., 2020. Determining fluoride distribution and influencing factors in groundwater in Songyuan, Northeast China, using hydrochemical and isotopic methods. J. Geochem. Explor. 217, 106605 https://doi.org/10.1016/j.gexplo.2020.106605.
Yidana, S.M., Ophori, D., Banoeng-Yakubo, B., Samed, A.A., 2012. A factor model to explain the hydrochemistry and causes of fluoride enrichment in groundwater from the middle voltaian sedimentary aquifers in the Northern Region, Ghana. ARPN J. Eng. Appl. Sci. 7 (1), 50–68.
Yin, S., Xiao, Y., Han, P., Hao, Q., Gu, X., Men, B., Huang, L., 2020. Investigation of groundwater contamination and health implications in a typical semi-arid basin of North China. Water (Switzerland) 12 (4). https://doi.org/10.3390/W12041137.
Yousefi, M., Ghoochani, M., Hossein, A., 2018a. Health risk assessment to fluoride in drinking water of rural residents living in the Poldasht city, Northwest of Iran. Ecotoxicol. Environ. Saf. 148, 426–430. https://doi.org/10.1016/j.ecoenv.2017.10.057.
Yousefi, M., Mohammadi, A.A., Yaseri, M., Mahvi, A.H., 2017. Epidemiology of drinking water fluoride and itscontribution to fertility, infertility, and abortion: an ecological study in westAzerbaijan Province, Poldasht County, Iran. Res. Rep. Fluoride 50, 343–353.
Yousefi, M., Yaseri, M., Nabizadeh, R., Hooshmand, E., Jalilzadeh, M., 2018b. Association of hypertension, body mass index, and waist circumference with fluoride intake; water drinking in residents of fluoride endemic areas, Iran Association of Hypertension, Body Mass Index, and Waist Circumference with Fluoride Intake; Wate. Biol. Trace Elem. Res. 185, 282–288. https://doi.org/10.1007/s12011-018-1269-2.
Yu, Q., 2016. Study on the Space-Time Evolution Characteristic of Groundwater in the High Plains Area of Jilin Province. Jilin University.
Zhai, Y., Lei, Y., Wu, J., Teng, Y., Wang, J., Zhao, X., Pan, X., 2017. Does the groundwater nitrate pollution in China pose a risk to human health? A critical review of published data. Environ. Sci. Pollut. Res. 24 (4), 3640–3653. https://doi.org/10.1007/s11356-016-8088-9.
Zhang, B., Hong, M., Zhang, B., 2007. Fluorine distribution in aquatic environment and its health effect in the Western Region of the Songnen Plain. Northeast China 379–386. https://doi.org/10.1007/s10661-006-9592-z.
Zhang, L., Huang, D., Yang, J., Wei, X., Qin, J., Ou, S., Zhang, Z., Zou, Y., 2017. Probabilistic risk assessment of Chinese residents' exposure to fluoride in improved drinking water in endemic fluorosis areas. Environ. Pollut. 222, 118–125. https://doi.org/10.1016/j.envpol.2016.12.074.
Zhang, B., Mei, H., Zhao, Y., Lin, X., Zhang, X., Dong, J., 2003. Distribution and risk assessment of fluoride in drinking water in the west plain region of Jilin Province, China. Environ. Geochem. Health 25 (4), 421–431. https://doi.org/10.1023/B:EGAH.0000004560.47697.91.
Zhang, Z., Xiao, C., Adeyeye, O., Yang, W., Liang, X., 2020. Source and mobilization mechanism of iron, manganese, and arsenic in groundwater of Shuangliao City, Northeast China. Water (Switzerland) 12 (2). https://doi.org/10.3390/w12020534.
Zhan, H., Bian, A., 2006. A method of calculating pumping induced leakage. J. Hydrol. 328 (3), 659–667. https://doi.org/10.1016/j.jhydrol.2006.01.010.
Zhao, L.J., Wang, P., Gao, Y.H., Sun, D.J., 2013. National annual monitoring report of drinking water-borne endemic fluorosis in 2010 and 2011. Chin. J. Endem. Dis. 32, 2 (In Chinese).
Zhiwu, B., 2009. Study on the Enrichment Laws and Influencing Factors of Arsenic and Fluoride in Groundwater in the Songnen Plain. Jilin University,.
Zoni, S., 2007. Neuropsychological testing for the assessment of manganese neurotoxicity. A Rev. A Propos. 830, 812–830. https://doi.org/10.1002/ajim.20518.